Journal of Advances in Modeling Earth Systems

RESEARCH ARTICLE
10.1029/2017MS001253

Key Points:
- Crop growth, development, and yield formation have been well represented in the Dynamic Land Ecosystem Model (DLEM-AG2.0)
- Simulated results for wheat, maize, and rice are well tested against both field observations and national yield survey in China
- DLEM-AG2.0 provides an integrated modeling tool for achieving sustainable agricultural system

Supporting Information:
- Supporting Information S1

Correspondence to:
H. Tian,
tianhan@auburn.edu

Citation:
Zhang, J., Tian, H., Yang, J., & Pan, S. (2018). Improving representation of crop growth and yield in the Dynamic Land Ecosystem Model and its application to China. *Journal of Advances in Modeling Earth Systems*, *10*, 1680–1707. https://doi.org/10.1029/2017MS001253

Received 5 DEC 2017
Accepted 21 MAY 2018
Accepted article online 29 MAY 2018
Published online 28 JUL 2018

Improving Representation of Crop Growth and Yield in the Dynamic Land Ecosystem Model and Its Application to China

Jingting Zhang[1,2], Hanqin Tian[1,2], Jia Yang[2], and Shufen Pan[2]

[1]Research Center for Eco-Environmental Sciences, State Key Laboratory of Urban and Regional Ecology, Chinese Academy of Sciences, Beijing, China, [2]International Center for Climate and Global Change Research, School of Forestry and Wildlife Sciences, Auburn University, Auburn, AL, USA

Abstract To accurately assess the roles of agriculture in securing food security and maintaining environmental sustainability, it is essential to improve the representation of crop growth, development, and yield formation in global land models that traditionally focus on energy, water, carbon, and nitrogen exchanges between land and the atmosphere. In this study, a process-based agricultural module has been coupled with the Dynamic Land Ecosystem Model (DLEM-AG2.0) for assessing how multiple environmental factors (climate change, atmospheric CO_2 concentration, tropospheric O_3, and nitrogen deposition) and human activities (land use/cover change, nitrogen fertilizer use, and irrigation) have affected the crop growth, development, yield, carbon (C), nitrogen (N), and water cycles in agroecosystems. Here we describe the model structure for simulating crop growth, development, and yield formation in the DLEM-AG2.0, and then we validate the model using field observations and a national yield survey for three major crops (wheat, maize, and rice) in China during 1980–2012. Results show that the DLEM-AG2.0 is capable of simulating the dynamic processes of phenological development, leaf growth expansion, biomass accumulation, biomass allocation, and yield formation for wheat, maize, and rice with normalized root mean square errors of the simulations of less than 20%. Our model-based yield estimation for the three major crops at the national scale for the period 1980–2012 is generally consistent with the national yield survey in China. The crop representation in the DLEM-AG2.0 is flexible for extrapolating to a global scale after rigorous testing with both site-specific and regional observations. Further advancement of agricultural modeling within the global land modeling framework will require consideration of human perception and behavior for adapting and mitigating global change.

1. Introduction

Agriculture plays controversial roles in increasing the food supply to meet the growing human demand (Borlaug, 2007) while also releasing large amounts of greenhouse gases to the atmosphere (Tian, Lu, et al., 2016). Humans have influenced 42–68% of the land surface through agriculture, wood harvesting, and grazing activities (Hurtt et al., 2006). Globally, approximately 12% of the land surface is currently used for the agricultural sector (Food and Agriculture Organization, 2017). Both natural and human-induced environmental changes have notably influenced crop growth and yield in intricate ways—interacting with each other and having a combined impact on the agricultural sector (Schindler, 2001). Conversely, agriculture can have a significant influence on climate change by altering the surface fluxes of greenhouse gases, albedo, and heat fluxes (Drewniak et al., 2013; Levis et al., 2012). For instance, irrigation and conservation tillage on croplands resulted in a regional or global cooling effect, exerting special strong effects on precipitation, cloud cover, and radiation (Cook et al., 2014; Diffenbaugh, 2009; Guimberteau et al., 2012; Lobell et al., 2006; Lobell & Field, 2007). However, emissions of non-CO_2 greenhouse gases (CH_4 and N_2O) from agriculture could totally offset the terrestrial carbon sink, warming the climate (Tian, Lu, et al., 2016). Thus, to fully understand the roles of agriculture in the climate system and food security, assessing and predicting crop production and its consequences on climate and the environment from an Earth system perspective are essential (Drewniak et al., 2013; McDermid et al., 2017).

Two separate modeling groups exist for simulating crop growth and yield. First, multiple decades of efforts in crop modeling have created a number of crop models such as EPIC (Erosion Productivity Impact Calculator; Cole et al., 1987), DSSAT (Decision Support System for Agrotechnology Transfer; Uehara & Tsuji, 1991), ORYZA

(Bouman et al., 2001), CERES (Crop Environment REsource Synthesis; e.g., Jones & Kiniry, 1986), and APSIM (Agricultural Production Systems sIMulator; Keating et al., 2003; Mccown et al., 1996). These crop models are good for quantifying crop physiological and phenological processes. For example, based on crop variety, climate, soil conditions, and management practices, the crop models are capable of simulating the dynamic of crop growth, development, seed formation, and yield (Okada et al., 2015). However, most of them (e.g., ORYZA, DSSAT, and APSIM) are site-based, farmer-oriented, and lacking in adequate representation of biogeochemical and hydrological cycles, and they rarely have been applied at regional or global scales.

Conversely, a number of large-scale regional and global land models have explored the effects of global change on crop growth and its feedback to climate through a simplistic representation of crops, such as generic crop-like grasses (sometimes distinguished by their photosynthetic pathways; Pitman et al., 2009). However, relative to grasslands, cropland has different biogeophysical and biogeochemical characteristics due to the agricultural managements (e.g., fertilizer and irrigation) and should include more realistic phenology (McDermid et al., 2017). To address the complexity of crop growth and biogeochemical cycles, much effort has been made to better represent agriculture in a global land modeling framework (Bondeau et al., 2007; Kucharik, 2003; Levis et al., 2012; Osborne et al., 2006; Ren et al., 2012; Smith et al., 2010). Some more sophisticated crop models have been incorporated into Earth system models. For instance, Osborne et al. (2006, 2009) performed global simulations by using the Hadley Centre Atmosphere Model, version 3 (HadAM3) with a crop model GLAM (General Large-Area Model for annual crops; a warm climate crop model) in the land component, to examine the interactive effect of crop phenology on tropical climate variability. However, the simulation did not include explicit residue management and crop organ development, which are major uncertainties in climate simulation (Drewniak et al., 2013; Iizumi et al., 2014; Levis et al., 2012). Recently, Drewniak et al. (2013) developed an approach to integrate agriculture representations for three crop types—maize, soybean, and spring wheat—into a coupled carbon-nitrogen version of the CLM (CLM-Crop; Community Land Model, Levis et al., 2012), which has added nitrogen cycling (nitrogen retranslocation, and soybean nitrogen fixation) and management practices (fertilizer and residue harvest). Leng et al. (2016) had used an improved CLM-Crop to simulate county-level crop yields by optimizing irrigation and fertilization in the United States.

Although these more advanced representations of crop growth in global land models have improved the simulation of agricultural ecosystems, some critical processes and drivers are still poorly represented, for example, (1) multifactor-driven changes in C fluxes and pools, (2) process-based crop phenology development and dynamic biomass allocation, and (3) crop rotation and tillage practices. These processes and drivers are underrepresented, in part, due to a lack of long-term large-scale spatial data sets of cropland management measures (including an irrigation and fertilizer application database); failure to combine land ecosystem model and process-based crop models; and the failure to consider multiple environmental factors. Therefore, to reduce uncertainty in estimating crop yields at a large scale, the development of a process-based crop module within global land models is needed, as well as using relevant regional databases to drive the models. The databases should include the major environmental factors that influence crop growth and development in the agroecosystems.

In this study, building on the previous version of the agricultural module in the Dynamic Land Ecosystem Model (DLEM-Ag, Ren et al., 2012; Tian et al., 2012), we have developed a new version of the DLEM-AG2.0 agroecosystem model, to help understand the impacts of multifactor environmental changes on crop growth, development, and yield. The DLEM-AG2.0 is a spatially explicit, process-based agroecosystem model representing the influences of agronomic practices and environmental factors on crop phenology, growth and development, yield, and biogeochemical and hydrological processes. It is capable of simulating the dynamic processes of phenological development, leaf area growth expansion, main growth stages, biomass accumulation, biomass allocation, and organ formation for wheat, maize, and rice, as well as the interactive effects of climate and soil on these crop yield and feedback processes. As a case study, we applied this new model version to China's cropland for verifying the model's ability to simulate crop growth and yield in the context of multiple environmental stresses. China's cropland accounts for approximately 7% of the world's arable land but supports 22% of the global population (Ren et al., 2012). In recent decades, China's agricultural ecosystems have been affected by a complex set of environmental stresses originating from climate, chemical composition of the atmosphere (e.g., CO_2, tropospheric O_3, and nitrogen deposition), land use and cover change, and agriculture management practices (e.g., fertilizer and irrigation uses; Tian, Melillo,

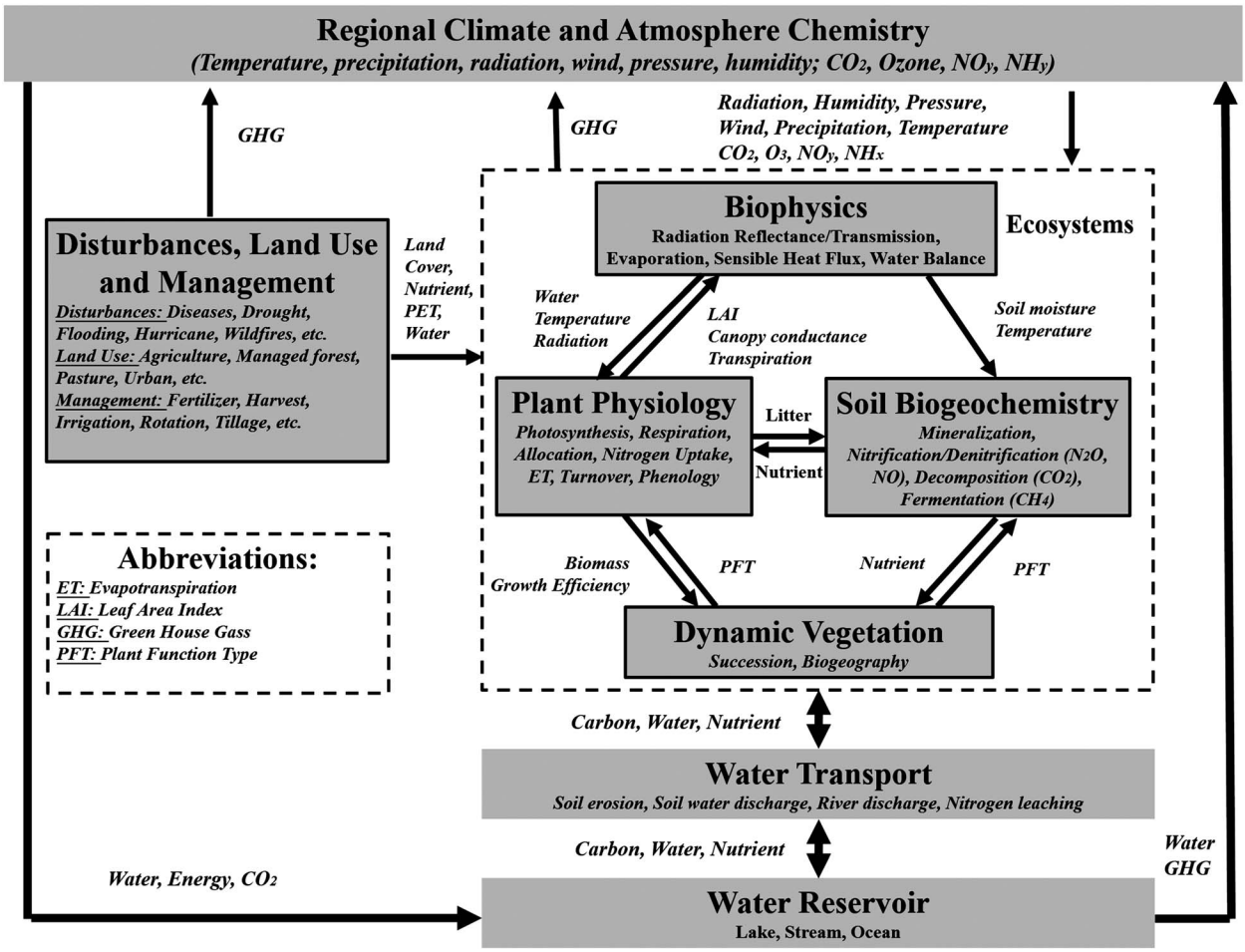

Figure 1. Key components of the Dynamic Land Ecosystem Model (DLEM) and its linkage to the climate and human systems (Tian, Liu, et al., 2010).

et al., 2011). As China is one of the most intensively studied regions in the world, substantial data sets on crop distribution, soil properties, farming practices, climate, and land use/cover change are available for building long-term and high-resolution regional databases (e.g., Lu & Tian, 2007; Ren et al., 2007; Yan et al., 2005). These data sets can be used to drive the DLEM-AG2.0 for simulating crop yield in responses to multiple environmental changes. Therefore, China is ideal for verifying our new agroecosystem model.

The purpose of this paper is to (1) provide detailed information on the DLEM-AG2.0 algorithms; (2) evaluate model performance against field observations of phenology, leaf area index (LAI), biomass, and yield at the site level; (3) examine responses of crop growth and yield to multiple environmental changes at the national level; and finally, (4) discuss uncertainty and future research needs in agroecosystem modeling and simulation.

2. The DLEM

The DLEM is a highly integrated, process-based terrestrial ecosystem model that simulates the structural and functional dynamics of terrestrial ecosystems affected by multiple factors, including climate, atmospheric composition (CO_2, nitrogen deposition, and tropospheric ozone), land use and cover change, and agriculture management practices (e.g., harvest, rotation, irrigation, and fertilizer use; Tian, Chen, et al., 2010; Tian, Liu, et al., 2010). The DLEM has five core components: (1) biophysics, (2) plant physiology, (3) soil biogeochemistry, (4) vegetation dynamics, and (5) land use and management (Tian, Chen, et al., 2010; Tian, Liu, et al., 2010). The DLEM simulation results have been extensively calibrated and validated using many field observations and measurements in typical vegetation types including forest, grassland, and cropland at the site level (Lu & Tian, 2013; Ren et al., 2011; Tao et al., 2014; Tian, Chen, et al., 2010; Tian, Melillo, et al., 2011). The DLEM-estimated fluxes and the storage of water, carbon, and nutrients have been compared with the

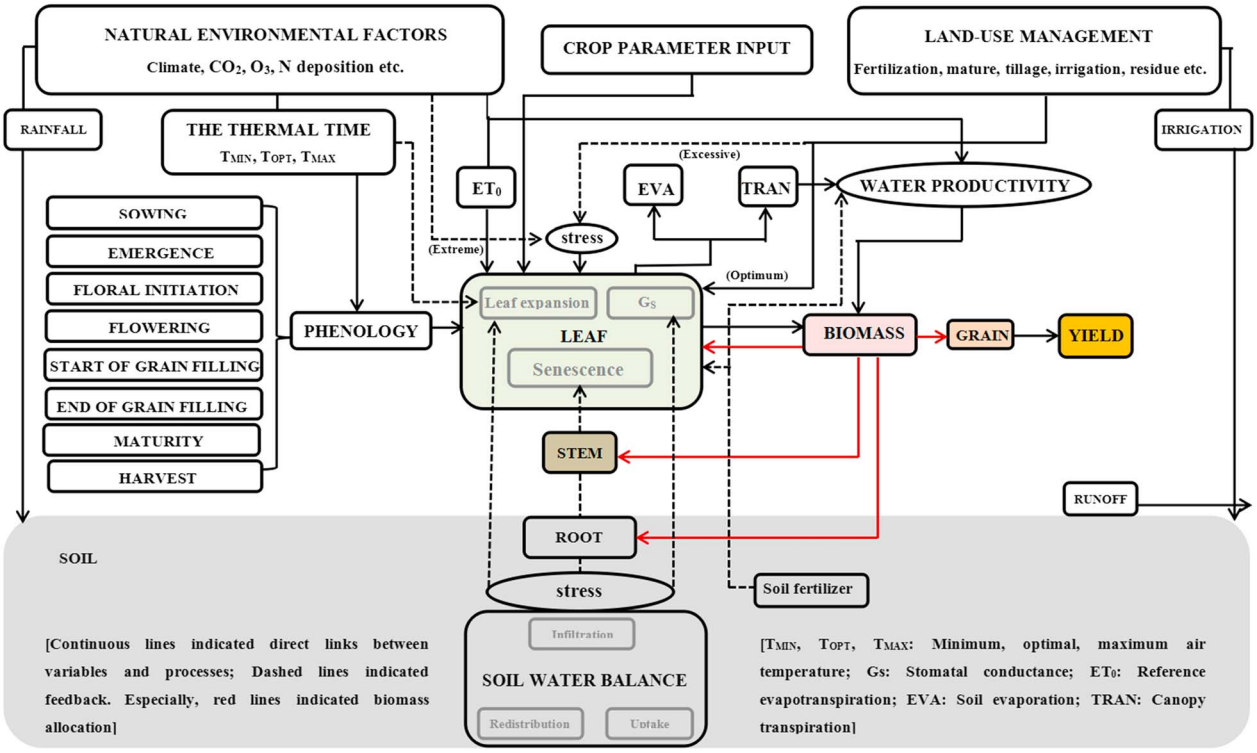

Figure 2. Framework of the agricultural module in Dynamic Land Ecosystem Model (DLEM-AG2.0). The conceptual framework describing the main components of the soil-plant-atmosphere continuum and the key parameters related to phenology, canopy cover, transpiration, biomass production, and final yield (Tmin, minimum temperature for photosynthesis; Topt, optimum temperature for photosynthesis; Tmax, maximum temperature for photosynthesis; ETo, reference evapotranspiration; EVA, soil evaporation; TRAN, canopy transpiration; Gs, stomatal conductance). Continuous lines indicate direct links between variables and processes. Especially, red lines indicate biomass allocation. Dashed lines indicate feedbacks.

estimates from other approaches, such as statistical-based empirical modeling, top-down inversion, or other process-based modeling approaches, at regional, continental, and global scales (Pan et al., 2014, 2015; Tian, Lu, et al., 2016; Tian, Ren, et al., 2016; Yang et al., 2014). The DLEM model has been used in China (Lu & Tian, 2007; Lu et al., 2012; Ren et al., 2007, 2012; Tian, Melillo, et al., 2011; Tian, Xu, et al., 2011), the United States (Song et al., 2013; Tian, Chen, et al., 2010; Tian et al., 2012), and North America (Tian, Chen, et al., 2015; Xu et al., 2010). The detailed information on how the DLEM simulates these processes is shown in Tian, Liu, et al. (2010). Recently, the model was updated to the DLEM 2.0 (Figure 1), which is characterized by the cohort structure; multisoil layer processes; coupled carbon, water, and nitrogen cycles; multiple GHG (CO_2, CH_4, and N_2O) emissions; enhanced land surface processes, such as vegetation dynamics and soil moisture movement, which improved the representation of the surface heterogeneity; and the dynamic linkages between terrestrial and riverine ecosystems (Liu, Evans, et al., 2013; Liu et al., 2008; Liu, Tian, et al., 2013; Pan et al., 2014, 2015; Tian, Ren, et al., 2016; Tian et al., 2014; Zhang et al., 2016). In this paper, we present the improved agroecosystem model (DLEM-AG2.0), which simulates crop growth and development responses to the natural environment (radiation, temperature, etc.), soil water and soil nitrogen, and management practices in a daily time step (Figure 2).

2.1. Development of the New Agroecosystem Model (DLEM-AG2.0)

The new version of the agroecosystem model (DLEM-AG2.0) was improved based on the previous DLEM-Ag module (Ren et al., 2011, 2012; Tian et al., 2012). Although the DLEM-Ag incorporated the influences of agronomic practices on crop growth and phenology and other biogeochemical processes (Ren et al., 2011, 2012; Tian, Ren, et al., 2016; Tian et al., 2012), the DLEM-Ag has not fully represented crop growth, development, allocation, seed formation, and yield. The improved version of DLEM-AG2.0 has adopted some key features from well-established crop models (e.g., EPIC, DSSAT, ORYZA, CERES, and APSIM; Bouman et al., 2001; Cole et al., 1987; Jones & Kiniry, 1986; Keating et al., 2003; Mccown et al., 1996; Uehara & Tsuji,

1991) as subsequently described. In DLEM-AG2.0, the natural vegetation and crops in a model grid can be simulated simultaneously.

The DLEM-AG2.0 simulates phenological development, leaf area growth, and C and N contents in the different parts of crop (leaf, stem, root, and grain) at a daily time step, and finally outputs the crop yield. Crop photosynthesis, growth, and development are controlled by multiple factors including climate (temperature, precipitation, solar radiation, and relative humidity), atmospheric chemistry (CO_2, O_3, N deposition, etc.), soil water and nutrient availability, and management practices (N fertilizer use, irrigation, tillage). Crop life cycle is separated into eight stages (i.e., sowing, emergence, floral initiation, flowering, start of grain filling, end of grain filling, maturity, and harvest) based on the accumulation of thermal time. Each stage is characterized by a different carbon allocation strategy, light use efficiency, and turnover rate. The biomass is allocated into different parts of the crop (leaf, stem, root, and grain) with varied allocation parameters during the different stages.

The DLEM-AG2.0 enhances the ability of the DLEM-Ag model to simulate crop phenology, biomass allocation, and yield formation (Figure 2). It aims to simulate crop growth and yield as well as carbon, nitrogen, and water cycles in agricultural ecosystems affected by multiple environmental factors. Other processes, such as crop growth (e.g., photosynthesis, respiration, and nitrogen cycle), soil biogeochemistry (e.g., decomposition, nitrification, and fermentation), and air pollution effect (e.g., O_3, see Text S4 in the supporting information, cited with Felzer et al., 2004, 2005; Ollinger et al., 1997; Reich, 1987) are simulated in the same way as in the DLEM-Ag. The detailed information of these processes has been described in our previously published papers (e.g., Lu et al., 2012; Lu & Tian, 2013; Pan et al., 2014, 2015; Ren et al., 2007, 2010, 2011; Tian, Chen, et al., 2010; Tian, Liu, et al., 2010; Tian, Melillo, et al., 2011; Tian, Xu, et al., 2011). However, in the DLEM-AG2.0, different crops are specifically parameterized according to each crop type. In addition to incorporating natural environmental driving factors, the module pays special attention to the role of agronomic practices, including irrigation, fertilization, and rotation on crop growth and soil biogeochemical cycles. The following sections describe the improved agricultural module in DLEM (DLEM-AG2.0) and its applications to China.

2.1.1. Phenology

The growth and development processes of crops are divided into eight growth stages, including sowing, emergence, floral initiation, flowering, start of grain filling, end of grain filling, maturity, and harvest (Figure S1 in the supporting information). The timing of each phase is determined by the accumulation of thermal time (ATT, °C day) adjusted by various impact factors (e.g., vernalization, photoperiod, and N). The length of each phase is determined by a fixed fraction of ATT (fATT), which is specified in the parameter table (Table 1). The fATT for each growth stage is calculated as follows:

$$\mathrm{ATT} = \sum \left[\mathrm{DTT} \times \min(f_D, f_V)\right] \tag{1}$$

$$\mathrm{fATT} = \frac{\sum_{\text{sowing}}^{\text{current day}} \mathrm{DTT}}{\mathrm{ATT}} \tag{2}$$

$$\mathrm{DTT} = \begin{cases} T_{\text{ave}} - \mathrm{Card}_{\min}, \mathrm{Card}_{\min} < T_{\text{ave}} \le \mathrm{Card}_{\text{opt}} \\ \left[\dfrac{(\mathrm{Card}_{\max} - T_{\text{ave}}) * (\mathrm{Card}_{\text{opt}} - \mathrm{Card}_{\min})}{(\mathrm{Card}_{\max} - \mathrm{Card}_{\text{opt}})}\right], \mathrm{Card}_{\text{opt}} < T_{\text{ave}} \le \mathrm{Card}_{\max} \\ 0, \qquad T_{\text{ave}} < \mathrm{Card}_{\min} \text{ or } T_{\text{ave}} > \mathrm{Card}_{\max} \end{cases}. \tag{3}$$

where DTT is the daily thermal time (°C day), which can be reduced by the genetic photoperiod factor (f_D) and vernalization factor (f_V); f_D and f_V are the same as in the APSIM model (Mccown et al., 1996; see Text S1 in the Supporting Information); T_{ave} is the average 2-m air temperature for the current day (°C); $\mathrm{Card}_{\min}$ is the minimum temperature required for photosynthesis (°C); $\mathrm{Card}_{\max}$ is the maximum temperature required for photosynthesis (°C); and $\mathrm{Card}_{\text{opt}}$ is the optimal temperature required for photosynthesis (°C; see Table 1), as in the APSIM model and the SWAT (Soil Water Assessment Tool) model (Neitsch et al., 2005).

First, the total ATT between the plant and harvest dates for each crop was calculated for every grid cell based on the 30-year average temperature from 1980 to 2010, using equations (1) and (3). The ATT maps vary with the crop species and grids. Then, for each crop, we set the different ATT targets necessary to reach each

Table 1
List of Major Parameter Values for Wheat, Maize, and Rice in China Used to Drive the DLEM-AG2.0

		Value in this study			Value range in other studies			
Parameter	Varietal Parameter	Wheat	Maize	Rice	Wheat	Maize	Rice	References
Control growth	Card_min (°C)	0	8	10	0–8	5–10	8–15	Lobell et al. (2012); Liu et al. (2016); Jone et al. (2003); Neitsch et al. (2005); McMaster et al. (2008); Mccown et al. (1996); Keating et al. (2003); Zhang et al. (2004); Luo (2011); Liu, Hubbard, et al. (2013); Sanchez et al. (2014)
	Card_opt (°C)	26	34	30	20–26	30–34	30–35	
	Card_max (°C)	34	44	43	30–34	40–44	38–43	
	fATT_emerg	0.05	0.06	0.04	0.03–0.08	0.03–0.07	0.03–0.05	Levis et al. (2012); Drewniak et al. (2013); Mohanty et al. (2012); Chen et al. (2010a, 2010b); Zhang et al. (2012); Liu, Hubbard, et al. (2013); Sun et al. (2016)
	fATT_floini	0.26	0.30	0.18	0.25–0.46	0.12–0.26	0.18–0.28	
	fATT_flower	0.55	0.42	0.36	0.50–0.70	0.27–0.55	0.35–0.50	
	fATT_startfill	0.62	0.58	0.57	0.59–0.77	0.38–0.65	0.57–0.70	
	fATT_endfill	0.98	0.97	0.96	0.90–0.97	0.93–0.99	0.96–0.99	
	fATT_mature	1.00	1.00	1.00	1.00	1.00	1.00	
	Default ATT (°C days)	1,910	1,650	2800	1,650–2,600	1,050–2,800	2,100–3,200	
	R_P	2.3	3.0	2.5		1.0–5.0		Mohanty et al. (2012); Chen et al. (2010a, 2010b); Zhang et al. (2012)
	R_V	1.5	—	—	1.0–5.0	—	—	
Control yield	Alloc_root	See Figure S2			Max: 30–55%	Max: 40–75%	Max: 35–65%	Mccown et al. (1996); Yu et al. (2006); Feng et al. (2007); Chen et al. (2010a, 2010b); Yang et al. (2010); CNERN (http://www.cnern.org/index.action); Liu, Li, et al. (2011); Levis et al. (2012); Zhang et al. (2012); Drewniak et al. (2013); Cai et al. (2013)
	Alloc_leaf				Max: 50–85%	Max: 60–75%	Max: 55–90%	
	Pgrainfill (mg dry weight grain^{-1} day^{-1})				Max: 2.3–6.0	Max: 9.0–12.0	Max: 2.0–2.8	
	Ngrain_stem (kernels/g stem)	25	100	80	23–33	80–150	65–90	
	Dens_crop (ind/m^2)	250	6.0	25	150–500	4.0–7.0	20–50	
	Maxlai	7.00	6.50	5.70	3.0–7.0	2.5–6.5	2.5–6.5	
	Max_grainweight (g dry weight/grain)	0.06	0.50	0.04	0.032–0.08	0.30–0.65	0.025–0.065	

Note. Card_min, Card_opt, and Card_max is minimum, optimum, and maximum temperature for photosynthesis (°C), respectively; fATT_emerg, fATT_floini, fATT_flower, fATT_startfill, fATT_endfill, and fATT_mature mean fraction of accumulated thermal time (ATT) to reach emergence, floral initiation, flowering, start of grain filling, end of grain filling, and maturity stages, respectively; default ATT represents the total number of ATT necessary to reach maturity (°C days); R_P represents the sensitivities to photoperiod; R_V means the sensitivities to vernalization. Alloc_root and Alloc_leaf are allocation fraction of new accumulated biomasses to root and leaf, respectively; Pgrainfill means potential rate of grain filling (mg dry weight grain^{-1} day^{-1}); Ngrain_stem represents grain number per gram stem dry weight (kernels/g stem); Dens_crop is crop density (ind/m^2); Maxlai means maximum leaf area index; Max_grainweight represents maximum weight of grain (g dry weight/grain).

growth stage, derived from the references (e.g., Chen et al., 2010a, 2010b; Liu, Hubbard, et al., 2013; Sacks et al., 2010; Zhang et al., 2012). Thus, the fATTs for each crop were calculated and specified in the parameter table (Table 1). Finally, in the model simulation, the crop growth required to reach each growth stage, determined by regional climatology for the years 1900–2012, was based on equations (1)–(3).

2.1.2. Photosynthesis

The crop photosynthesis process in the DLEM-AG2.0 is the same as that for natural vegetation in the DLEM 2.0 version (Pan et al., 2014, 2015; Tian, Chen, et al., 2010; Tian, Liu, et al., 2010). The gross primary productivity (GPP) in the DLEM was calculated by scaling the leaf assimilation rates (g C m^{-2} day^{-1}) up to the whole canopy (Farquhar et al., 1980; Collatz et al., 1991; Bonan, 1996; Sellers et al., 1996).

$$\mathrm{GPP}_{\mathrm{sun}} = 12.01 \times 10^{-6} \times A_{\mathrm{sun}} \times \mathrm{plai}_{\mathrm{sun}} \times \mathrm{dayl} \times 3,600 \tag{4}$$

$$\mathrm{GPP}_{\mathrm{shade}} = 12.01 \times 10^{-6} \times A_{\mathrm{shade}} \times \mathrm{plai}_{\mathrm{shade}} \times \mathrm{dayl} \times 3,600 \tag{5}$$

$$\mathrm{GPP} = \mathrm{GPP}_{\mathrm{sun}} + \mathrm{GPP}_{\mathrm{shade}} \tag{6}$$

where $\mathrm{GPP}_{\mathrm{sun}}$ and $\mathrm{GPP}_{\mathrm{shade}}$ are the GPP of sunlit and shaded canopy, respectively; A_{sun} and A_{shade} are the assimilation rates of sunlit and shaded canopy, respectively; $\mathrm{plai}_{\mathrm{sum}}$ and $\mathrm{plai}_{\mathrm{shade}}$ are sunlit and shaded leaf area indices, estimated as equations in Text S2 in the supporting information, respectively; dayl is the

daytime length (s), and 12.01 $\times 10^{-6}$ is a constant to change the unit from μmol CO_2 to g C. The major parameters in estimating photosynthesis are listed in Table S1 in the supporting information.

Using similar methods to Collatz et al. (1991), the DLEM determines the C assimilation rate (A) as the minimum of three limiting rates—w_c, w_j, w_e—which are functions that represent the assimilation rates as limited by the efficiency of the photosynthetic enzymes system (Rubisco-limited), the amount of photosynthetically active radiation captured by the leaf chlorophyll (light-limited), and the capacity of leaves to export or utilize photosynthesis products (export-limited) for C_3 species, respectively. For C_4 species, w_e refers to the phosphoenolpyruvate carboxylase limited rate of carboxylation. The detailed information (cited with Bonan, 1996; Saxton & Rawls, 2006; Asseng et al., 1998; Bernacchi et al., 2001; Detmann et al., 2012; Drewniak et al., 2013; Evans & Poorter, 2001; Farquha et al., 1980; Hund et al., 2005; Levis et al., 2012; Pan et al., 2014, 2015; Rebetzke et al., 2004; Ren et al., 2012; Zhang et al., 2016) is in Text S2 in the supporting information

2.1.3. Respiration

The process of crop respiration is also the same as that for natural vegetation in the DLEM 2.0 version (Pan et al., 2014, 2015). The model estimates two types of respiration, which are maintenance respiration (Mr, g C m^{-2} day^{-1}) and growth respiration (Gr, g C m^{-2} day^{-1}). The Gr is calculated by assuming that the fixed part of assimilated C will be used to construct new tissue (for turnover or plant growth). During these processes, it is supposed that 25% of assimilated C (gross primary productivity, GPP) will be released back into the atmosphere as growth respiration (Ryan, 1991). After the carbon consumed by tissue maintenance and plant growth respiration has been subtracted, the remaining carbon is the net primary productivity (NPP, g $C/m^{2)}$.

$$\mathrm{Gr} = 0.25\mathrm{GPP} \tag{7}$$

$$\mathrm{NPP} = \mathrm{GPP} - \mathrm{Gr} - \mathrm{Mr} \tag{8}$$

Maintenance respiration is positively related to the temperature. The following equation is used to calculate the maintenance respiration of leaf, sapwood, fine root, and coarse root:

$$\mathrm{Mr}_i = R_{\mathrm{coeff}\_i} \times N_i \times f(T_{\mathrm{ave}}) \tag{9}$$

where i denotes the C pool of the different plant parts (leaf, sapwood, fine root, coarse root, or reproduction); Mr_i (g C m^{-2} day^{-1}) is the maintenance respiration of the pool i; R_{coeff_i} is a plant functional type-specific respiration coefficient of plant part i (cited with Gifford, 1995; Pan et al., 2014, 2015; Ren et al., 2012; Zhang et al., 2016); N_i (g N/m^2) is the nitrogen content of pool i (for crop, is N_{root}, N_{leaf}, N_{stem}, and N_{grain}, respectively); and $f(T_{\mathrm{ave}})$ is the temperature factor and is calculated as follows:

$$f(T_{\mathrm{ave}}) = e^{308.56 \times \left(\frac{1}{56.02} - \frac{1}{T_{\mathrm{ave}} + 46.02}\right)} \tag{10}$$

where T_{ave} is the daily average air temperature (°C) for modeling aboveground C pools such as the leaves, sapwood, and heartwood or soil temperature for modeling belowground pools such as coarse roots and fine roots.

2.1.4. Allocation

The assimilated carbon deducted by respiration is the rest of the carbon (namely, NPP), which is ready to be allocated to the different tissues. In DLEM-AG2.0, the crop is divided into four components or parts: the root, grain, leaf, and stem. The daily carbon increment (ΔC) forms the total daily accumulated biomasses (ΔQ) of the crop. Based on the allocation rule, daily accumulated biomasses (ΔQ) are used to update the root biomasses and then partition to the (1) grain, then (2) the leaf (proportion of the remaining biomasses), and, finally, the (3) stem.

a. Biomass Partitioning to the Root

All biomasses in the root are considered the structural fraction, which cannot be retranslocated later to other parts.

$$\Delta Q_{\mathrm{root}} = 2.0 \times \mathrm{ptoroot} \tag{11}$$

$$\mathrm{ptoroot} = \Delta \mathrm{C} \times \mathrm{rho} \tag{12}$$

$$\text{rho} = 3 \times \frac{L_{\text{light}}}{L_{\text{light}} + 2\left(\text{Min}\left(W_{\text{water}}, N_{\text{nitrogen}}\right)\right)} \times \text{Alloc\_root} \tag{13}$$

$$L_{\text{light}} = \text{Max}(\exp(-\text{ext}_{\text{coef}} \times \text{LAI}), 0.01) \tag{14}$$

$$W_{\text{water}} = \text{Max}(\text{btrans}, 0.01) \tag{15}$$

$$N_{\text{nitrogen}} = \text{Max}(f(N), 0.01) \tag{16}$$

$$f(N) = \min\left(\frac{N_{\text{leaf}}}{N_{\text{leaf\_opt}}}, 1\right) \tag{17}$$

where ΔQ_{root} is the daily increment in the root biomasses (g m^{-2} day^{-1}); ptoroot is the daily accumulated root carbon (g C m^{-2} day^{-1}); ΔC is the daily newly accumulated carbon (g C m^{-2} day^{-1}); rho is the fraction of the carbon allocated to the root; Alloc_root is the allocation fraction of the newly accumulated carbon to the root (0–1), which is a cultivar-specific parameter in Table 1; L_{light} is the scalar light available; W_{water} is scalar water available; N_{nitrogen} is the scalar available nitrogen; $f(N)$ is a nitrogen factor that affects grain filling; LAI is the actual leaf area, which is determined by the same calculation process as that of the natural vegetation in the DLEM 2.0 version (Pan et al., 2014; Tian, 2002; Tian, Liu, et al., 2010); btrans is the water limitation factor on evapotranspiration, which is calculated by soil water content (Pan et al., 2014; Tian, 2002; Tian, Chen, et al., 2010); N_{leaf} is the actual leaf nitrogen concentration; and $N_{\text{leaf\_opt}}$ is the optimal leaf nitrogen concentration for photosynthesis (g N/m^2), which is calculated based on leaf carbon content and the minimum leaf CN ratio ($CN_{\text{min, leaf}}$; Table S1 in the supporting information; Pan et al., 2014; Tian, 2002; Tian, Liu, et al., 2010). The ext_{coef} is the canopy light extinction coefficient, which is a cultivar-specific parameter in the parameter table (Table S1 in the supporting information, refer from Awal et al., 2005; Calderini et al., 1997; Dingkuhn et al., 1999; Flénet et al., 1996; Lunagaria & Shekh, 2006; Shearman et al., 2005). In the DLEM-AG2.0, nitrogen cycling is the same as that for natural vegetation in the DLEM 2.0 version (e.g., Lu et al., 2012; Lu & Tian, 2013; Ren et al., 2011; Tian, Xu, et al., 2011). The DLEM partitions C and N cycles into vegetation, litter, soil, microbe, and product components (Figure S3 in the supporting information). The N processes are closely coupled with the C processes in the biomass compartment through the specific C:N ratios. The N cycle is fully open; that is, the N in the ecosystem can be exchanged in external sources and sinks through deposition, leaching, nitrous gas emissions, and others. Detailed processes can be found in the Text S3 in the supporting information (cited with Asseng et al., 1998, 2011; Liu et al., 2008; Lu et al., 2012, 2013; Porter & Gawith, 1999; Rasterrer et al., 1997; Ren et al., 2007, 2011, 2012; Xu et al., 2010; Tian, Chen, et al., 2010; Tian, Liu, et al., 2010; Tian, Mellillo, et al., 2011; Tian, Xu, et al., 2011; Wang & Engel, 2002; Zhang et al., 2007, 2016).

b. Biomass Partitioning to the Grain

Next, all or part of the available biomasses are partitioned into grains according to actual demand of the grain.

$$\Delta Q_{\text{grain}} = 2.0 \times \text{ptoprod} \tag{18}$$

$$\text{ptoprod} = \text{Min}\left(\Delta C_{\text{grain}} \times 0.8, D_g^{'}\right) \tag{19}$$

$$\Delta C_{\text{grain}} = \Delta C - \text{ptoroot} \tag{20}$$

$$D_{\text{g}}^{'} = \begin{cases} 0, & \Delta C_{\text{grain}} > D_{\text{gm}}; \\ \min\left(D_{\text{grain}}, D_{\text{gm}} - \Delta C_{\text{grain}}\right), & \Delta C_{\text{grain}} \le D_{\text{gm}}; \end{cases} \tag{21}$$

$$D_{\text{grain}} = \text{Den\_crop} \times \text{Ngrain\_plant} \times \text{Pgrainfill} \times 0.5 \times f(N) \times \text{ftair} \tag{22}$$

$$D_{\text{gm}} = \text{Den\_crop} \times \text{Ngrain\_plant} \times \text{Max\_grainweight} \times 0.5 \tag{23}$$

$$\text{Ngrain\_plant} = \begin{cases} 0, & \text{crop stage} < 5; \\ \text{Ngrain}_{\text{stem}} \times \text{Cstem}_{\text{anthesis}} \times 2.0, & 5 \le \text{crop stage} \le 8; \end{cases} \tag{24}$$

$$\text{For wheat, ftair} = \begin{cases} 0, & T_{ave} < 0 \text{ or } T_{ave} > 45; \\ \dfrac{T_{ave}}{26.0}, & 0 \le T_{ave} \le 26; \\ 1.0, & 26 < T_{ave} \le 35; \\ \dfrac{45.0 - T_{ave}}{10.0}, & 35 < T_{ave} \le 45; \end{cases}$$

$$\text{For maize, ftair} = \begin{cases} 0, & T_{ave} < 6 \text{ or } T_{ave} > 56.3; \\ \dfrac{(T_{ave} - 6) \times 0.4}{4.0}, & 6 \le T_{ave} \le 10; \\ \dfrac{(T_{ave} - 10) \times 0.35}{6.0} + 0.4, & 10 < T_{ave} \le 16; \\ \dfrac{(T_{ave} - 16) \times 0.25}{6.0} + 0.75; & 16 < T_{ave} \le 22; \\ 1.0; & 22 < T_{ave} \le 30; \\ 1.0 - \dfrac{T_{ave} - 30.0}{26.3}, & 30 < T_{ave} \le 56.3; \end{cases} \quad (25)$$

$$\text{For rice, ftair} = \begin{cases} 0, & T_{ave} < 10 \text{ or } T_{ave} > 43; \\ 0.1 \times (T_{ave} - 10.0), & 10 \le T_{ave} \le 20; \\ 1.0, & 20 < T_{ave} \le 37; \\ 1.0 - \dfrac{1.0}{6.0 \times (T_{ave} - 37.0)}, & 37 < T_{ave} \le 43; \end{cases}$$

where ΔQ_{grain} is the daily available biomass for the grain (g m^{-2} day^{-1}); ptoprod is the allocated grain carbon (g C m^{-2} day^{-1}); ΔC_{grain} is the daily newly accumulated carbon for the grain (g C m^{-2} day^{-1}); D_g' (g C m^{-2} day^{-1}) is the actual demands for grain limited by the potential grain demands (D_{grain}, g C m^{-2} day^{-1}) and the maximum grain size (corresponding to D_{gm}, g C m^{-2} day^{-1}); D_{grain} is calculated in the post-flowering growth phase (from flowering to the end of grain filling); Den_crop is the crop density (plant/m^2, Table 1); Ngrain_plant is the number of grains per plant (grain/plant, Table 1); *Pgrainfill* is the potential rate of grain filling (g dry weight $grain^{-1}$ day^{-1}, Table 1); ftair is a function of daily mean temperature, which affects the rate of grain filling (0–1); Max_grainweight is the maximum weight of grain (g dry weight/grain, which is a cultivar-specific parameter in Table 1; $Ngrain_{stem}$ is the grain number per gram of the stem dry weight (grain number/g), which is a cultivar-specific parameter in Table 1; and $Cstem_{anthesis}$ is the allocated stem carbon from the anthesis stage to the harvest (g/plant).

c. Biomass Partitioning to the Leaf

The remaining biomasses (after the partitioning to the grains) are partitioned into the leaf based on a stage-dependent function. Leaf biomasses are considered as structural and thus cannot be remobilized.

$$\Delta Q_{leaf} = 2.0 \times \text{ptoleaf} \quad (26)$$

$$\text{ptoleaf} = \Delta C_{leaf} \times \text{Alloc\_leaf} \quad (27)$$

$$\Delta C_{leaf} = \Delta C - \text{ptoroot} - \text{ptoprod} \quad (28)$$

where ΔQ_{leaf} is the daily increment in the leaf biomasses (g m^{-2} day^{-1}); ptoleaf is the allocated leaf carbon (g C m^{-2} day^{-1}); ΔC_{leaf} is the daily newly accumulated carbon for the leaf (g C m^{-2} day^{-1}); and Alloc_leaf is the allocated fraction of the available biomasses partitioned to the leaf (0–1), which are set values for the different crop types, as shown in Table 1.

d. Biomass Partitioning to the Stem

The whole remaining biomasses (if any) are partitioned into the stem. Until the stage "start of grain filling," 65% ($h_{structural}$) of these biomasses are allocated to structural biomasses, whereas the remaining 35% are

allocated to the nonstructural biomasses. Afterward, all new biomasses allocated to the stem are for nonstructural biomasses (which can remobilized).

$$\Delta Q_{\text{stem}} = 2.0 \times \text{ptostem} \tag{29}$$

$$\text{ptostem} = \Delta C - \text{ptoroot} - \text{ptoprod} - \text{ptoleaf} \tag{30}$$

$$\Delta Q_{\text{stem.structural}} = \Delta Q_{\text{stem}} \times h_{\text{structural}} \tag{31}$$

$$\Delta Q_{\text{stem.non-strucutural}} = \Delta Q_{\text{stem}} \times (1 - h_{\text{structural}}) \tag{32}$$

where ΔQ_{stem} is the daily increment in the stem biomasses (g m^{-2} day^{-1}); ptostem is allocated to the stem carbon (g C m^{-2} day^{-1}); $\Delta Q_{\text{stem. structural}}$ is allocated to the stem structural biomasses (g m^{-2} day^{-1}); $\Delta Q_{\text{stem. non - strucutural}}$ is allocated to the stem nonstructural biomasses (g m^{-2} day^{-1}); and $h_{\text{structural}}$ is the percentage of remaining biomasses allocated to the stem structural biomasses.

2.1.5. Tissue Turnover

For a crop, the daily leaf-turnover rate is zero until the mature stage, and the reproduction turnover rate is zero until the harvest stage. Other tissue turnover is similar to that of the natural plants in DLEM 2.0 (Tian, 2002; Tian, Liu, et al., 2010). Three main causes of leaf turnover are as follows: age (ftleaf_age), heat stress (ftleaf_heat), and water stress (ftleaf_drought).

$$\text{ftleaf\_age} = 1/(\text{ftleaf} \times 365) \tag{33}$$

$$\text{ftleaf\_drought} = \text{ftleaf\_sen\_water} \times (1 - \text{btrans}) \tag{34}$$

$$\text{ftleaf\_heat} = \begin{cases} 0, & \text{Tmax} < \text{tair1}; \\ \dfrac{0.05 \times (\text{Tmax} - \text{tair1})}{\text{Max}((\text{tair2} - \text{tair1}), 0.0001)}, & \text{tair1} \le \text{Tmax} \le \text{tair2}; \\ \dfrac{0.05 + 0.35 \times (\text{Tmax} - \text{tair2})}{\text{Max}((\text{tair3} - \text{air2}), 0.0001)}, & \text{tair2} \le \text{Tmax} \le \text{tair3}; \\ 0.4, & \text{Tmax} > \text{tair3}; \end{cases} \tag{35}$$

$$\text{ftleaf\_all} = \text{Min}(1, \text{Max}(\text{ftleaf\_age}, \text{ftleaf\_drought}, \text{ftleaf\_heat})) \tag{36}$$

$$\text{ltlfc} = \sum_{\text{sowing date}}^{\text{harvest date}} (\text{ptoleaf}) \times \text{ftleaf\_all} \tag{37}$$

where ftleaf is the leaf turnover time (year); ftleaf_sen_water is the slope of the linear equation relating to the soil water stress to the leaf senescence rate (see Table S1 in the supporting information, refer from Boonjung & Fukai, 1996; Steduto et al., 2009; Wolfe et al., 1988); ftleaf_age is the fraction of the leaf turnover rate caused by the plant age; ftleaf_drought is the fraction of the leaf turnover rate caused by the water stress; Tmax is the daily maximum temperature (°C); tair1, tair2, and tair3 are the three temperatures to define the heat-induced leaf turnover rate (°C, Table S1 in the supporting information, refer from Lobell et al., 2012; Liu et al., 2016; Jone et al., 2003; Neitsch et al., 2005; McMaster et al., 2008; McCown et al., 1996; Keating et al., 2003; Zhang et al., 2004; Sharkey, 2005; Luo et al., 2011; Liu, Hubbard, et al., 2013; Sanchez et al., 2013); ftleaf_heat is the fraction of leaf turnover rate caused by heat stress; and ltlfc is the leaf turnover carbon in the growing season (g C m^{-2} day^{-1}).

At the day of harvest, all grain is harvested. The harvested biomasses are as follows:

$$c_{\text{harv}} = \sum_{\text{start of grain filling}}^{\text{harvest date}} \text{ptoprod} \tag{38}$$

$$Q_{\text{harv}} = 2.0 \times c_{\text{harv}} \tag{39}$$

For the crop residue, part is removed from the field due to management, such as with fire; the other part is allocated to litter pools. The biomasses of the litter pools during harvest are calculated as follows:

$$\text{lc}_{\text{harv}} = (C_{\text{veg}} - c_{\text{harv}}) \times (1 - \text{fremov}) \tag{40}$$

where C_{veg} is the total vegetation biomasses; lc_{harv} is the carbon left from harvest; fremov is the carbon/nitrogen loss percentage (%, nongrain residue returned to litter pool) for the part of the residues

lost due to management (e.g., fire), which is a cultivar-specific parameter and is set as 30% in the parameter table (Table S1 in the supporting information, refer from Drewniak et al., 2013).

2.2. Input Data

Several sets of georeferenced input data (0.25° × 0.25°) are compiled to drive the DLEM-AG 2.0 model, including the following (see Figures S4–S6):

1. Climate. Daily climate data (maximum, minimum, and mean air temperature; precipitation; relative humidity; and downward shortwave radiation) during the period 1900–2012 were derived from the Climate Research Unit—National Center for Environmental Prediction six-hourly climate data sets (http://dods.extra.cea.fr/store/p529viov/cruncep/V4_1901_2012/readme.htm).
2. Atmospheric chemical components (atmospheric CO_2 concentration, AOT_{40} O_3 index, and nitrogen deposition). Atmospheric CO_2 concentration data were obtained from a spline fit of the Law Dome before 1959 (http://cdiac.ornl.gov/ftp/trends/co2/lawdome.smoothed. yr20) and from NOAA (http://www.esrl.noaa.gov/gmd/ccgg/trends/global. html) during the period 1959–2012. Monthly atmospheric ozone concentration was represented by AOT_{40} (Felzer et al., 2005) and further interpolated to daily data (Tian, Ren, et al., 2016). Atmospheric nitrogen deposition data were obtained from the North American Carbon Program Multi-scale Synthesis and Terrestrial Model Intercomparison Project (Wei et al., 2014).
3. Soil properties (soil texture, soil pH, and bulk density). The basic soil physical and chemical properties, such as the soil texture, bulk density, and soil pH, were obtained from the Harmonized World Soil Database (Wieder et al., 2014). The soil columns were separated for agricultural vegetation and natural vegetation.
4. Land use and land cover data. Cropland distribution was derived from the 5-arc min resolution HYDE v3.1 data and aggregated to 0.25° (Goldewijk et al., 2011). The main crop categories in each grid were first identified according to the global crop geographic distribution map (Leff et al., 2004) and were then refined based on census data from Food and Agriculture Organization of the United Nations Statistics Division and the Chinese Academy of Agricultural Sciences (http://www.caas.net.cn). Cropland distribution data set is on a yearly time step. We focused on 15 major crops in China that are representative of both dry farmland and paddy fields of C_3 and C_4 plants, including maize (spring and summer maize), rice (early, single, and late rice), wheat (winter and spring wheat), soybean, barley, cotton, peanut, naked oat, potato, rapeseed, sugarbeet, sorghum, sugarcane, sunflower, and millet. During the same period, we assumed that only one crop type (the largest planting percentage) exists in a grid. For rotation practices, we assumed that the fallow period between the growing seasons of two crops is more than 7 days. The plant and harvest dates for each crop were derived from more than 770 agricultural meteorological stations in China, which were from the Chinese Academy of Agricultural Sciences (http://www.caas.net.cn) and the China Meteorological Data Center (http://data.cma.cn/user/toLogin.html). Each county in China has only one agriculture meteorological station, with an observational period from 1980 to present for most stations. The observed variables include the cropping system, crop growth duration, yield, management, disaster, soil physical properties, soil moisture, climate, and others for each major crop type. To interpolate the station data to 0.25° spatial resolution for use in DLEM-AG 2.0, we made several assumptions. For the counties with observational data, we assumed that the plant and harvest dates for each crop type in a grid cell are the same with observational data for each county. For those counties lacking agriculture meteorological stations, we assumed that crop plant and harvest dates were the same with those in the nearest counties that have the same cropping systems. More detailed method was based on Monfreda et al. (2008).
5. Agricultural management practices (irrigation, nitrogen fertilizer use, and rotation). Nitrogen fertilizer use rates for China were derived from county-level census data (Tian, Yang, et al., 2015; Tian et al., 2012) and Food and Agriculture Organization country-level statistical data (http://faostat3.fao.org/download/E/EF/E). We use fertilizer data sets to establish spatial fertilizer application by crop type according to the method of Potter et al. (2010). An irrigation map was also developed from the survey database at both county and provincial levels for different crops. We assumed that the soil moisture would reach field capacity when irrigated and that the irrigation amount is determined when the soil moisture of the top layer drops to 30% of the maximum available water (i.e., field capacity minus wilting point) during the growing season in the identified irrigated grids (Ren et al., 2011). We used two major cropping systems, including the single cropping system and double cropping system (summer maize-winter wheat, rice-winter wheat, early

rice-late rice, and wheat-rapeseed). Because the cropping system is very important in China and directly influences estimations of crop production, a contemporary rotation map was developed. The rotation type in each grid was developed based on phenological characteristics derived from multitemporal remote sensing images at 1-km spatial resolution (Yan et al., 2005), which was then aggregated into 0.25° resolution referencing the field observations from the Chinese Academy of Agricultural Sciences (http://www.caas.net.cn) and China Meteorological Data Center (http://data.cma.cn/user/toLogin.html; see Figure S6).

6. Other ancillary data, such as river network and topographic data. Further details of other input data can be found in previous publications (Ren et al., 2011; Tian, Chen, et al., 2015; Tian, Yang, et al., 2015; Xu et al., 2010; Yang et al., 2014; Zhang et al., 2016).

2.3. Model Parameterization, Calibration, and Validation

The DLEM-AG2.0 had been parameterized, calibrated, and validated using field data collected from the National Ecosystem Research Network of China (CNERN, http://www.cnern.org/index.action) and from the literature (e.g., Cai et al., 2013; Ding et al., 2007; Jing et al., 2007; Liu, Zhang, et al., 2012; Liu, Qu, et al., 2012; Mo et al., 2012; Wei et al., 2007; Yu et al., 2006; Zhao et al., 2010; Figure S7). To simulate a crop, the DLEM-AG2.0 requires generic crop parameters that describe the growth and development characteristics and yield processes parameters (Table 1). We first used the calculated parameters to run the model, and then we refined the parameter values to get a better match between the simulated and measured values. Based on the agroecosystem experimental observations and other research results (Asseng et al., 1998; Chen et al., 2010a, 2010b, 2016; Holzworth et al., 2014; Liu & Tian, 2010; Mohanty et al., 2012), the thermal time between the various crop growth stages could be estimated. Genetic coefficients were determined after obtaining a close match between the observed and predicted values for LAI, total biomasses, grain yield, time to reach physiological maturity, etc. Fine-tuning was usually accomplished within a ±20% range of first-estimated values. The parameter values that resulted in minimal bias between the simulated and measured values at all sites were selected. After calibration, these coefficients were used in the subsequent model validation (section 3.1).

To test model performance against independent data, we chose part of site-level data for calibration and the other part for validation (section 3.1). The details on these agroecosystem experimental observations information have been documented in Tables S2–S4 (cited with Cai et al., 2013; Cui et al., 2012; Ding et al., 2007; Dong et al., 2011; Feng et al., 2007; Han et al., 2013; Hu et al., 2016; Jing et al., 2007; Li et al., 2003; Liu, Li, et al., 2011; Liu, Qu, et al., 2012; Liu, Wang, et al., 2011, Liu, Zhang, et al., 2012; Liu et al., 2014, 2015; Ma et al., 2013; Mo et al., 2011, 2012; Pan et al., 2014; Wei et al., 2007; Xiao et al., 2005; Yang et al., 2010, 2015; Yu et al., 2006; Zhai et al., 2011; Zhao et al., 2010; Zhang et al., 2013, etc.) in the supporting information. For wheat, cultivars used in calibration were the most popular winter wheat cultivars in Northern China Plain (winter wheat-maize rotation system, Shandong, Hebei, and Henan), one of the most widely grown winter wheat cultivar in the semiarid area of Northern China (continuous cropping, Shaanxi), and the predominant spring wheat cultivars in the semiarid area of Northern China (single cropping, Inner Mongolia). The DLEM-AG 2.0 was parameterized for maize in three typical agroecosystems, including a winter wheat-maize rotation system (Shandong, Hebei, and Henan), spring maize single cropping system (Heilongjiang), and spring maize continuous cropping system (Shaanxi and Gansu). The observation data derived from single rice (Hailun, Heilongjiang), rice-winter wheat rotation (Jiangpu, Jiangsu), and double rice (Changsha, Hunan) were used to parameterize for rice in DLEM-AG 2.0. Measured and simulated LAI, biomass of organs, and yield were compared graphically and analyzed statistically (Loague & Green, 1991).

Statistical indicators were used to evaluate the model performance, such as Student's t test ($P(t^*)$), the regression coefficient (β), the coefficient of determination (R^2), the root mean square error (RMSE), and the normalized root mean square error (NRMSE) between simulated and measured values. A model reproduces experimental data best when R^2 is close to 1, $P(t^*)$ is less than 0.05, RMSE is similar to the standard deviation of measured variables, and NRMSE is of the same order of magnitude as the coefficient of variance of the measured variables. The simulation is considered excellent with NRMSE $<$ 10%, good if 10–20%, acceptable if 20–30%, and poor if $>$30% (Jamieson et al., 1991).

After the parameter values had been repeatedly calculated and refined to get a better match between simulated and measured values, the final major parameter values that describe the growth and development characteristics and yield processes for the running model were determined and are listed in Table 1. Based

Table 2
Experimental Design

	Climate (CLM)	CO_2	Ozone (O_3)	Nitrogen deposition (Ndep)	Land use and cover change (LUCC)	Nitrogen fertilizer (Nfer)
Reference	1900–1930	1900	1900	1900	1900	1900
All combined	1901–2012	1901–2012	1901–2012	1901–2012	1901–2012	1901–2012

Note. CLM, CO_2, O_3, Ndep, LUCC, and Nfer are abbreviations for climate, atmospheric CO_2 concentration, atmospheric O_3 concentration, N deposition, land use and cover change, and N fertilization, respectively. The time period indicates that driver data (e.g., climatic data and atmospheric chemistry data) were being used in those periods.

on these parameter values, the DLEM-AG2.0-estimated LAI, aboveground biomasses (g/m^2), and dry grain weight (g/m^2) for wheat, maize, and rice in representative sites agree well with the observed values (Figures S8–S10). For wheat, the RMSE (NRMSE) for the LAI (Figure S8a), aboveground biomasses (Figure S8b), and dry grain weight (Figure S8c) were 0.57 (8.4%), 95.96 (6.3%), and 117.25 g/m^2 (10.8%), respectively. For maize, the RMSEs (NRMSEs) were 0.52 (7.6%), 121.13 (7.1%), and 113.84 g/m^2 (9.6%), respectively (Figure S9). For rice, the RMSEs (NRMSEs) were 0.52 (7.6%), 121.13 (7.1%), and 113.84 g/m^2 (9.6%), respectively (Figure S10). The overall R^2 ranged from 0.89 to 0.97 for the wheat, maize, and rice. Therefore, the DLEM-AG2.0 simulated LAI, aboveground biomasses, and grain yield dynamics are good fit with observation data at these calibrated sites in China.

2.4. Model Simulation

After the model validation, to evaluate crop yields, we tested a scenario experiment (see Table 2): all-combined (climate, CO_2, O_3, N deposition, land use and cover change, and N fertilizer) multifactor changes. The "all-combined" scenario would be close to typical agroecosystems in a relatively real world.

The model simulation at the country level follows a two-step procedure: an equilibrium simulation and a transient simulation. The model simulation begins with an equilibrium stage with long-term average climate data for the period 1900–1930 and 1900 levels of atmospheric CO_2 concentrations and vegetation cover. The equilibrium run is performed for 20,000 years at most or until the net carbon exchange between the atmosphere and the region is less than 0.1 g C/m^2, the change in soil water pool is less than 0.1 mm, and the change in soil total nitrogen content is less than 0.1 g N/m^2 between two consecutive 10-year periods. Finally, the model was fed by the time series of input data set in the transient mode. The model was run at a daily time step for simulating crop development and growth. Data were analyzed using analysis of variance, and tests of significance were done using a *t* test (Gomez & Gomez, 1984). The significant differences among treatments were compared with the critical difference at the 5% level of probability.

3. Results

3.1. Model Performance of Crop Growth and Yield Simulations at Site Level

To validate the performance of the DLEM-AG2.0 simulations, we have focused on three key indexes for each crop: the LAI, aboveground biomasses (g/m^2), and dry grain weight (g/m^2).

3.1.1. Leaf Area Index

The DLEM-AG2.0-estimated LAI was compared with observed data from wheat, maize, and rice, as shown in Figure 3. The RMSEs (NRMSEs) of wheat (Figure 3a), maize (Figure 3b), and rice (Figure 3c) were 0.59 (8.5%), 0.76 (11.1%), and 0.54 (8.2%), respectively. The R^2 ranged from 0.88 to 0.92 (n = 73–279). The simulated peak LAI for the wheat and maize is generally consistent with field observations at both the Yucheng and Luancheng sites (Figure 4). However, because the LAI decline is overestimated in the model, the LAI values are lower than observations in the late growth period. This causes lower grain biomass in the late growth stages, producing lower yields than observed because less carbon is assimilated in the simulation.

The LAI in the model is controlled by the amount of carbon in the leaves and a constant specific leaf area (SLA; the ratio of leaf area to dry leaf weight) for the different crop types. However, Tardieu et al. (1999) and Amanullah et al. (2007) indicate that the SLA varies throughout the growing season and is affected by

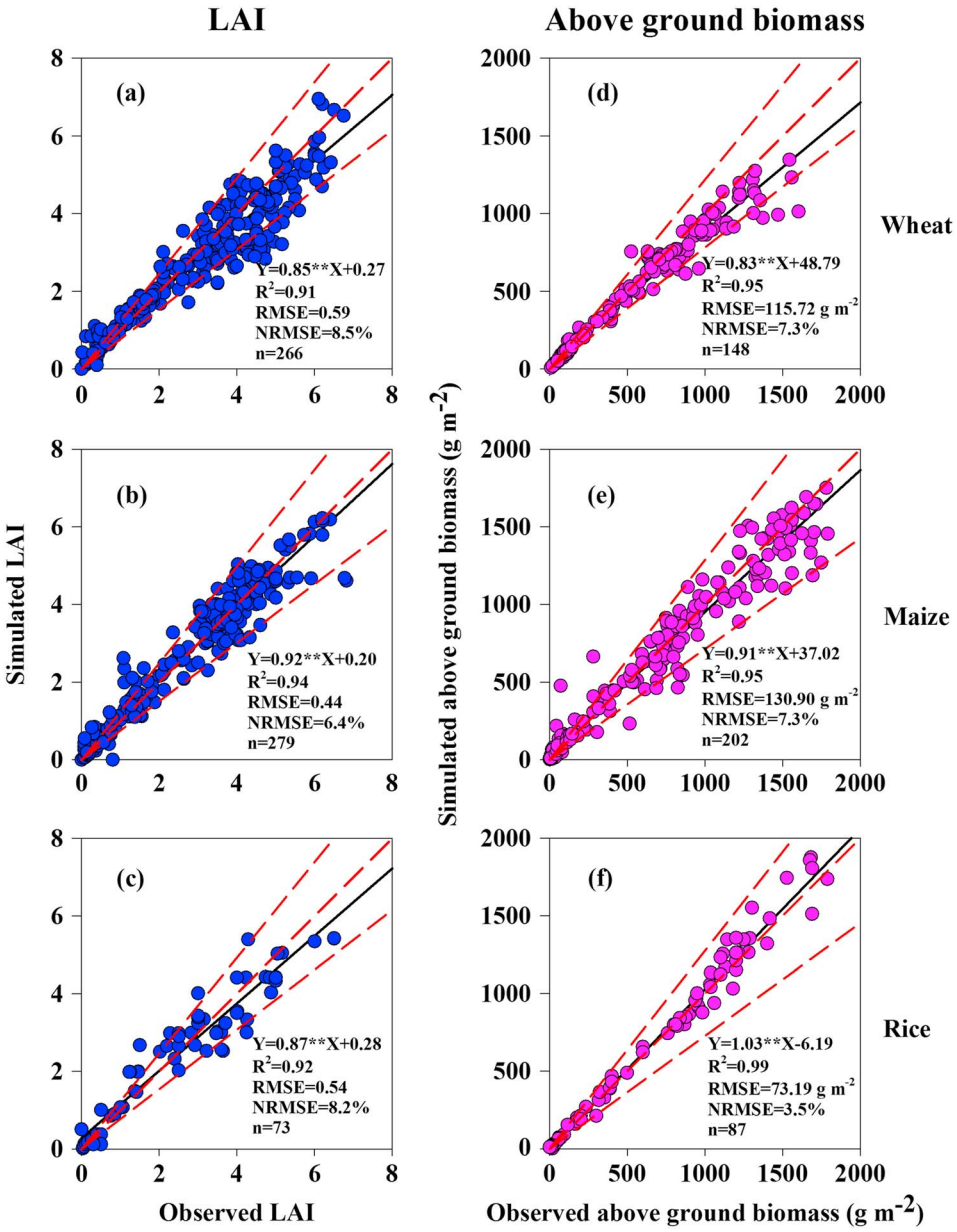

Figure 3. Comparison of the DLEM-AG2.0-estimated leaf area index (LAI) and aboveground biomasses with the observed data for wheat (a, b), maize (c, d), and rice (e, f). The solid line represents the regression line. The dotted lines represent the 1:1 line and 95% confidence intervals. RMSE = root mean square error, NRMSE = normalized root mean square error.

nitrogen fertilizer and climate change. Varying SLA during the growth period is not simulated in the DLEM-AG2.0, causing discrepancies between the observations and the simulations.

3.1.2. Biomass

The DLEM-AG2.0 simulated aboveground biomasses for wheat (Figure 3d), maize (Figure 3e), and rice (Figure 3f) were consistent with the field observations. The RMSE (NRMSE) ranged from 73.19 to 130.90 g/m^2 (3.5% to 7.3%), and the R^2 ranged from 0.95 to 0.99 (n = 87–202). Although the aboveground biomasses modeled well in the early growing season, the peaks at higher values were lower than observations made after the grain fill stage (Figure 5). The result might be due to two reasons. First, less photosynthate was produced because simulated LAIs were lower than observations in the late growth period. Second, when nitrogen was limited for grain development, simulated aboveground biomasses decrease later in the growing season.

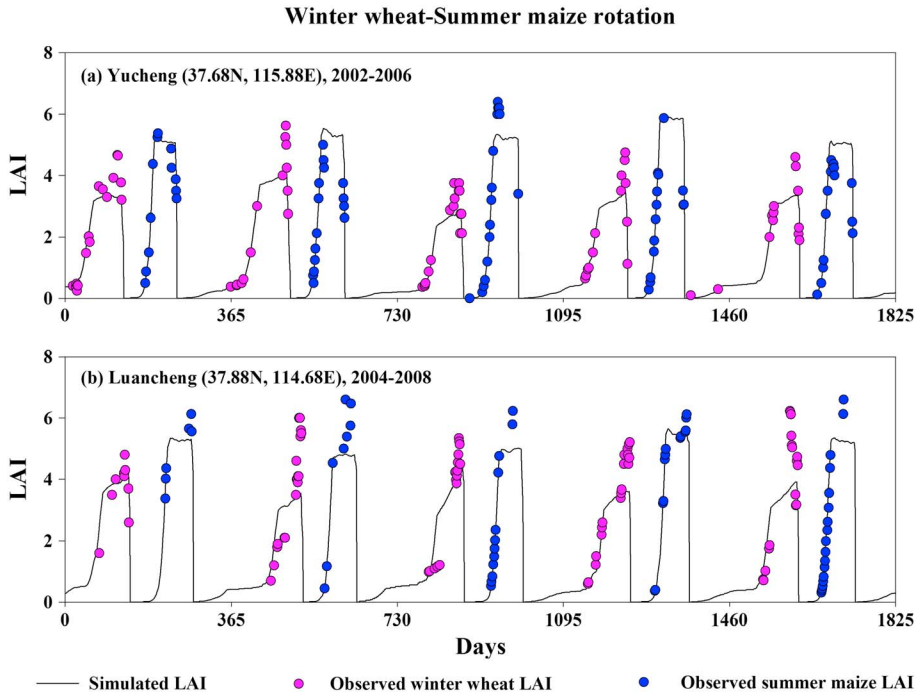

Figure 4. Comparisons of the simulated and the measured leaf area index (LAI) for wheat and maize from 2002 to 2006 (a) at Yucheng station and 2004–2008 (b) at Luancheng station.

The total aboveground biomass in the leaves, stems, and grains of the wheat, maize, and rice are shown in Figure 6. For wheat, the NRMSE ranged from 4.7% to 9.2% and the R^2 ranged from 0.86 to 0.96 (n = 72–134; Figures 6a–6c). For maize, the NRMSE ranged from 6.9% to 15.3%, and the R^2 ranged from 0.80 to 0.94 (n = 79–133; Figures 6d–6f). For rice, the NRMSE ranged from 7.1% to 8.2%, and the R^2 ranged from

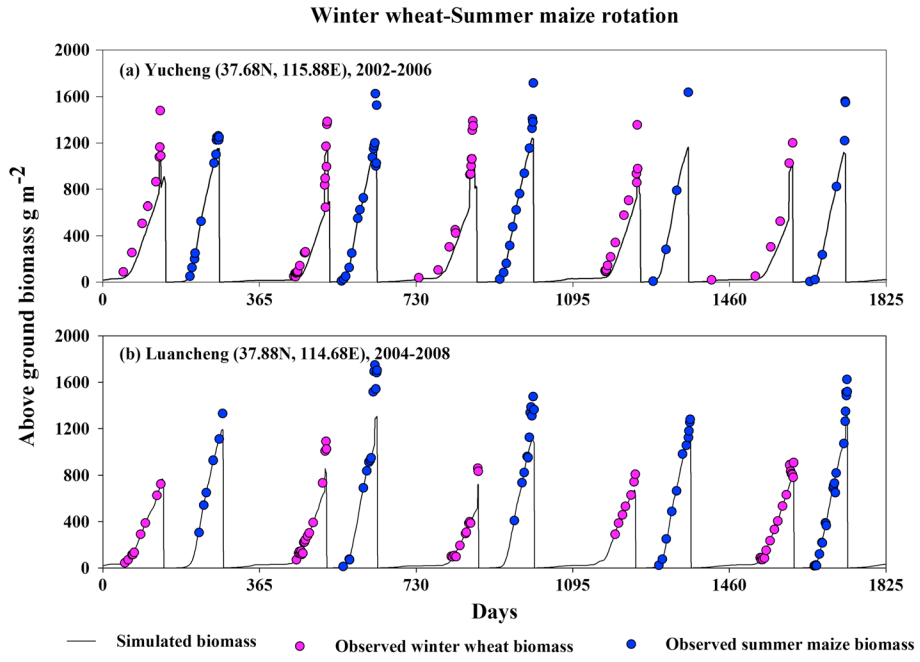

Figure 5. Comparisons of the simulated and the measured aboveground biomasses for wheat, maize, and rice at (a) Yucheng station (2002–2006) and (b) Luancheng station (2004–2008), respectively.

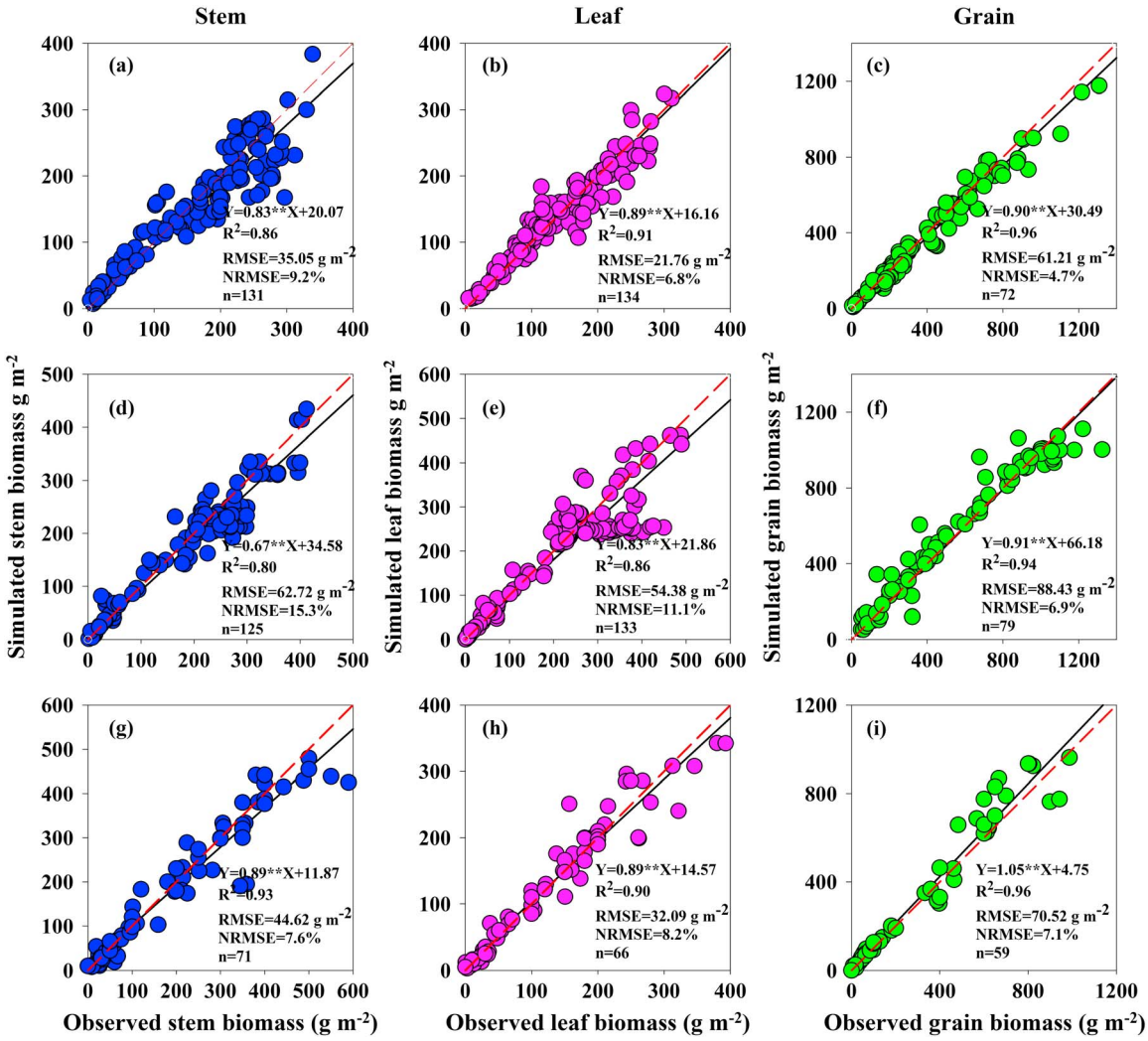

Figure 6. Comparison of DLEM-AG2.0-estimated stem, leaf, and grain biomass with the observed data for wheat (a, b, c), maize (d, e, f), and rice (g, h, i), respectively. The solid line represents the repetitive line. The dotted lines represent the 1:1 line. RMSE = root mean square error, NRMSE = normalized root mean square error.

0.90 to 0.96 (n = 59–71; Figures 6g–6i). Overall, the NRMSE for the simulated biomasses was less than 20%, indicating the simulated stem, leaf, and grain biomasses for wheat, maize, and rice were generally consistent with observations. However, the leaf biomasses in three crops are underestimated by the model because nitrogen stress constrains growth since grain filling stage, in contrast to field observations (Figure 7). Biomasses in the stem were comparable with observations during the growing season, whereas the grain biomasses were underestimated. Because grain development relies on retranslocated carbon/nitrogen from leaves and stems, which is not included in the current version of DLEM-AG2.0, the lower organ carbon than observations is not surprising (Figure 7).

3.1.3. Yield

The DLEM-AG2.0-simulated yield for wheat, maize, and rice agreed well with observations (Figure 8). The RMSE (NRMSE) of the wheat (Figure 8a), maize (Figure 8b), and rice (Figure 8c) were 563.95 (15.1%), 885.07 (12.4%), and 940.74 kg ha^{-1} (10.8%), respectively. The R^2 ranged from 0.66 to 0.81 (n = 35–53). The discrepancies between the observed and simulated yields were very likely attributed to the decline in the LAI and limited nitrogen. Thus, better simulation of LAI and N cycle will help improve model simulation for crop yield.

3.2. Model Estimation and Evaluation of Crop Yield at National Level During the Period 1980–2012

The DLEM-AG2.0-based estimation indicates that the average annual crop yields in China for the period from 1980 to 2012 were 9.0×10^{10}, 1.2×10^{10}, 11.9×10^{10}, 12.8×10^{10}, and 4.7×10^{10} kg for winter wheat, spring

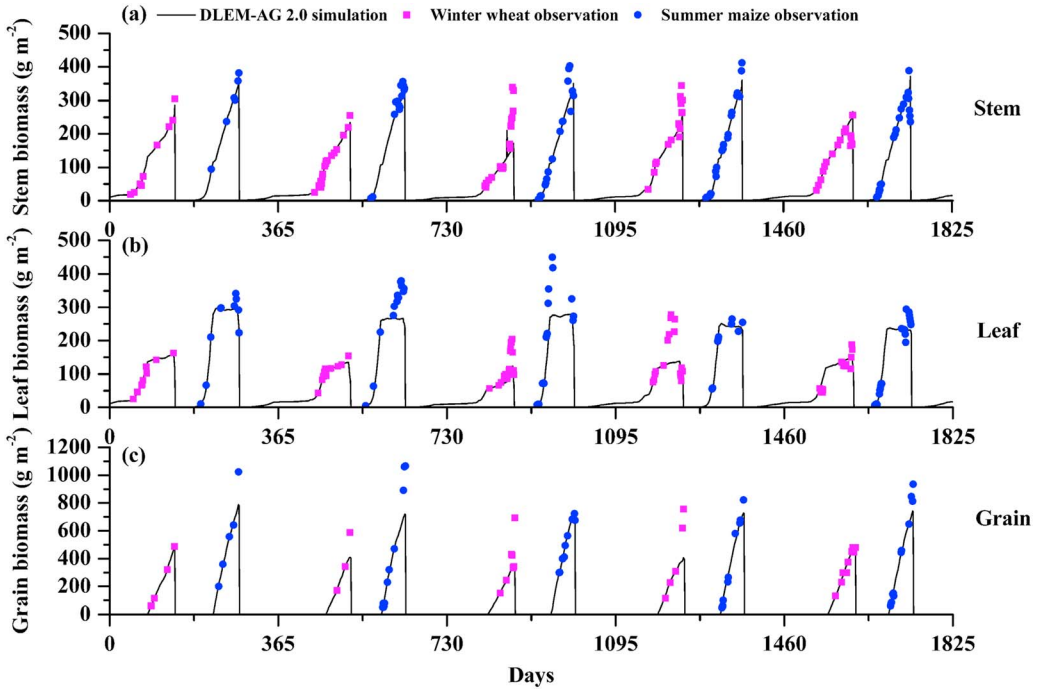

Figure 7. Comparisons of the simulated and the measured stem (a), leaf (b), and grain (c) biomasses for the winter wheat-summer maize rotation at Luancheng station (2004–2008).

wheat, maize, rice, and late rice, respectively (Table 3). Comparison between the DLEM-AG2.0-simulated average annual crop yields and the Ministry of Agriculture of the People's Republic of China statistics (http://zzys.agri.gov.cn/nongqingxm.aspx) is shown in Figure 9. The DLEM-AG2.0-simulated median yields agreed with observed yields for all crops. Both maize and wheat were overestimated, perhaps due to the lack of insect damage and disease analysis in the model. However, the full range of simulated yields for maize and wheat fell within the range of the observed yields. The range of simulated rice yields was spread larger than the observed values, and the median is slightly lower than the observed median yields. The yield has a significant dependence on fertilizer rates both in the model and in the field. DLEM-AG2.0 underestimated rice yield likely as a result of much higher fertilizer use in some region than those in the model.

In general, simulated annual yields for winter wheat, spring wheat, maize, rice, and late rice in China were consistent with observations (Figure 10). The RMSE (NRMSE) of the simulated yields for these crops was 889.7×10^7

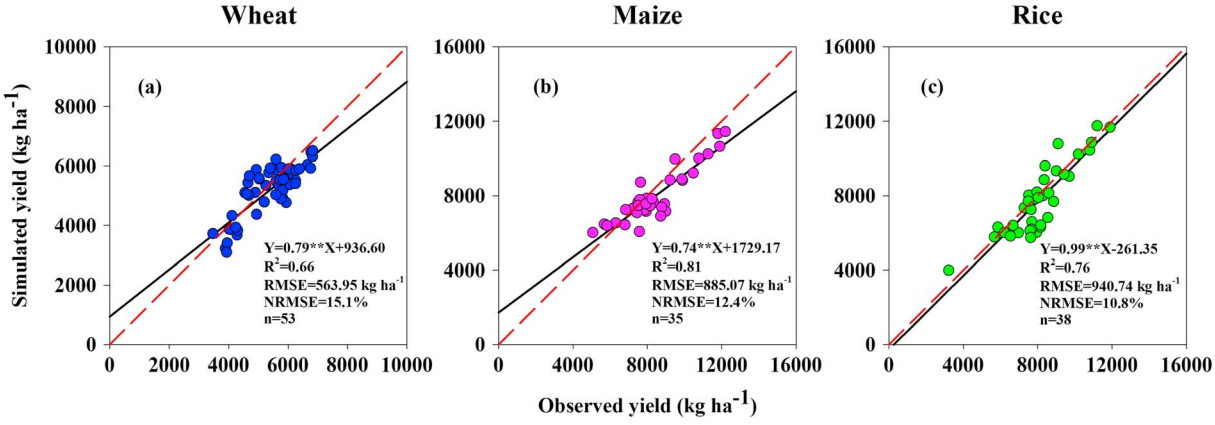

Figure 8. Comparison of DLEM-AG2.0-estimated yield with the observed data for wheat, maize, and rice. The solid line represents the repetitive line. The dotted lines represent the 1:1 line. RMSE = root mean square error, NRMSE = normalized root mean square error.

Table 3
Mean (10^7 kg) and the Trend (10^7 kg/year) of Annual Yields for Wheat, Maize, and Rice in China During 1980–2012

	Maize		Winter wheat		Spring wheat		Rice		Late rice	
Year	Mean	Trend	Mean	Trend	Mean	Trend	Mean	Trend	Mean	Trend
1980s	9,845.19	314.69*	7,361.21	275.41*	1,086.44	32.28*	10,390.98	348.56*	3,770.06	125.40*
1990s	12,135.67	52.55	9,370.07	24.50	1,208.65	−14.53	12,795.58	103.03*	4,709.52	85.39*
2000s	13,217.48	61.29	9,993.04	5.69	1,175.02	15.28	14,535.16	74.66	5,229.95	0.66
1980–2012	11,910.80	154.72*	9,044.87	119.31*	1,164.51	6.43*	12,781.88	188.15*	4,662.22	70.12*

Note. The asterisks indicate statistical significance at 0.95 level (*$p < 0.05$).

(17.6%), 98.1 × 10^7(16.3%), 1,069.4 × 10^7(16.4%), 1,441.9 × 10^7(19.3%), and 476.4 × 10^7 (17.6%)kg, respectively (Figure 10). The trends of the DLEM-AG2.0-simulated yields for winter wheat, spring wheat, maize, rice, and late rice were 119.3 × 10^7, 6.4 × 10^7, 154.7 × 10^7, 188.2 × 10^7, and 70.1 × 10^7 kg/year, respectively (Figure 10). The difference in the trend between the observed and simulated yields was insignificant ($p > 0.05$).

3.3. Regional Variability in Crop Yield

The DLEM-AG2.0-estimated average yields for wheat (winter wheat, and spring wheat), maize, and rice (early rice + single rice, late rice) showed a significant temporal-spatial change during the last 30 years (Figures 10–13 and Figures S11–S12). The interannual yield of wheat, maize, and rice in China was shown in Figure 10, which was caused mainly by variations in the climate, atmospheric chemical components (e.g., CO_2 concentration), and agricultural management practices (e.g., fertilization, land use, and cover change). In general, frequent rainfall, higher CO_2 concentration, and appropriate fertilizer allow the model to simulate higher yields. For winter wheat, higher yields (4,000–6,000 kg/ha) were distributed mainly in the winter wheat-summer maize rotation regions of Northern China Plain and winter wheat-rice rotation regions of Jiangsu and Yunnan provinces; less than 4,000 kg/ha of yields were associated with the semiarid regions (Shaanxi, Gansu, and Ningxia provinces) and the Southwestern mountainous regions (Guizhou and Sichuan provinces; Figure 11). For spring wheat, most regions showed a ranged of 0 to 2,000 kg/ha (Figure S11). For maize, the spring maize regions of the Northeast Plain showed a yield of 4,000–6,000 kg/ha, Xinjiang province and the semiarid area showed a yield of less than 4,000 kg/ha, and the highest yields were located in the southern regions (Figure 12). For rice (early + single rice), the Northeast Plain and the Southwestern regions (Guizhou and Yunnan provinces) showed the highest yield, with more than 6,000 kg/ha; the southern regions showed a yield ranging from 4,000 to 6,000 kg/ha (Figure 13). The yield of late rice over the southern regions was 4,000–6,000 kg/ha (Figure S12). Although the simulated yield at regional level is generally consistent with the provincial and national yield

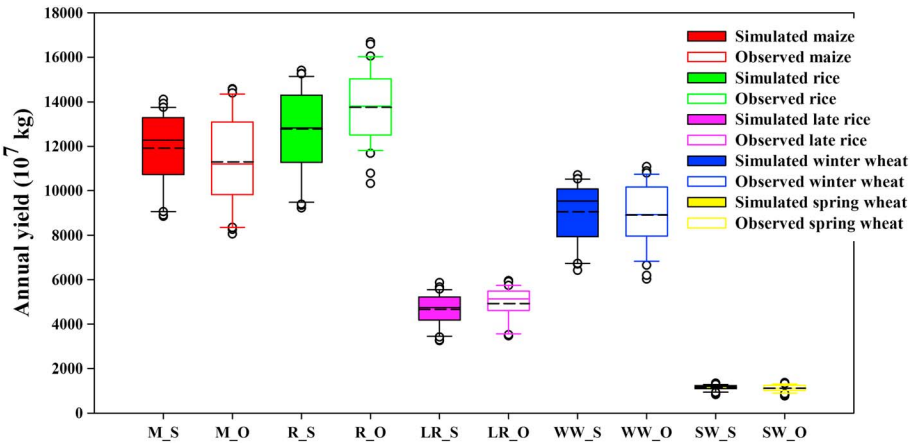

Figure 9. DLEM-AG2.0-simulated (filled) and the observed (unfilled; data from the Ministry of Agriculture of the People's Republic of China) yields for maize (M_S, M_O), rice (R_S, R_O), late rice (LR_S, LR_O), winter wheat (W_S, W_O), and spring wheat (SW_S, SW_O) in China. The box plots show the 10, 25, 50, 75, and 90 percentiles of annual yield. The dotted lines represent mean value.

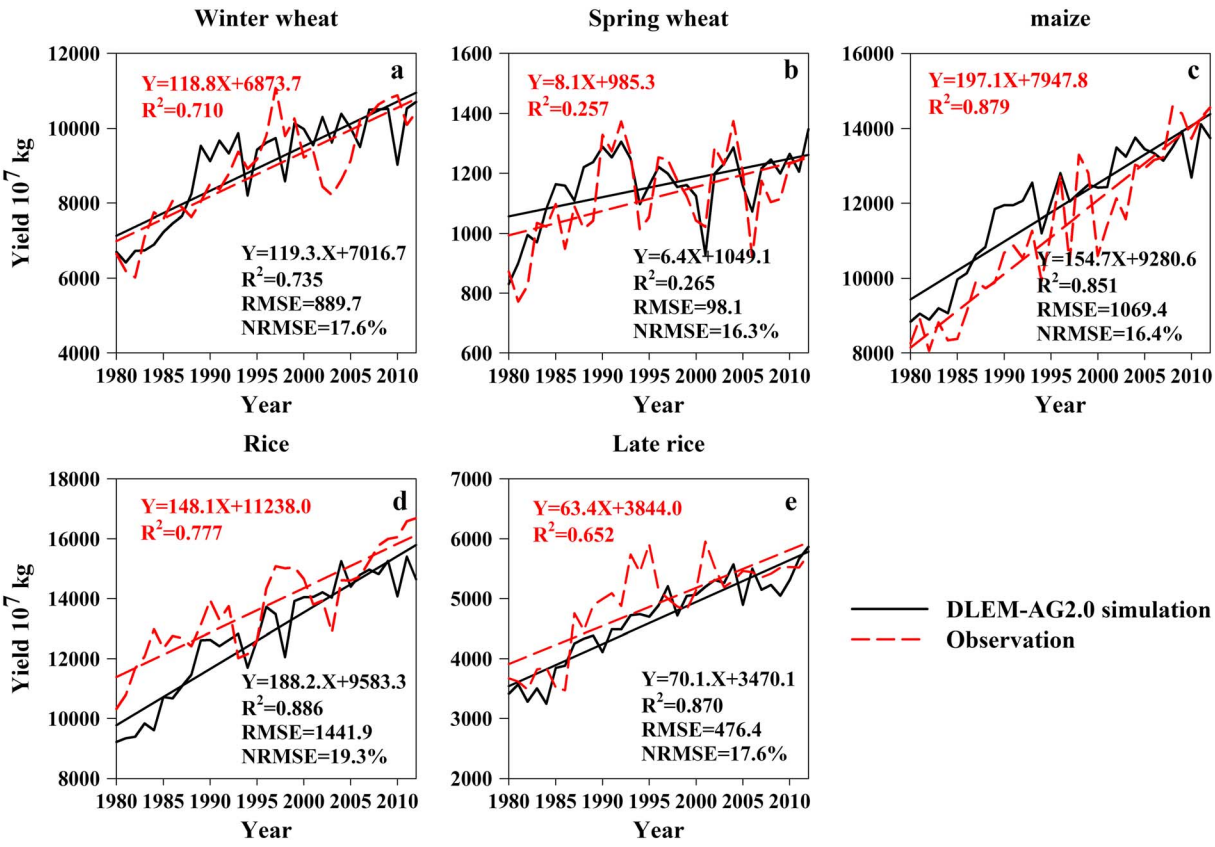

Figure 10. Comparisons of the simulated and the measured yield trend for winter wheat (a), spring wheat (b), maize (c), rice (d), and late rice (e) from 1980 to 2012. RMSE = root mean square error, NRMSE = normalized root mean square error.

surveys, direct spatial comparison of yields with observations is difficult because DLEM-AG2.0 simulation in this study runs at a relatively coarse spatial resolution, and high spatial resolution yield data across China are currently not available for such a data-model comparison.

4. Discussion

4.1. Effects of Environmental Factors on Crop Yield

As the various environmental stresses tend to interact with each other and exert a combined impact on the agroecosystem, natural and human-induced environmental changes have significantly influenced crop yields in complex ways (Felzer et al., 2005; Ren et al., 2012; Schindler, 2001; Tao et al., 2009). Previous studies have proved a positive correlation between yields and the atmospheric CO_2 concentration, atmospheric N deposition, and land use and cover change, whereas a negative correlation has been observed among the yield, climate change, and O_3 concentration (e.g., Aunan et al., 2000; Holland et al., 1997; Neff et al., 2000; Ren et al., 2007; Schindler & Bayley, 1993). Nitrogen deposition/fertilizer application could result in increases in crop yield in nitrogen-limited agroecosystems (Matson et al., 2002; Neff et al., 2000; Saleque et al., 2004; Swarup & Singh, 1989; Wang et al., 2003; Zhou et al., 2011) or could lead to a yield reduction in nitrogen-saturated ecosystems (Magill et al., 2000; Swarup & Singh, 1989; Zhou et al., 2011). However, the effect of a single factor could be enhanced or could be weakened. The direction of the response could be reversed by its interactions with other environmental factors (Ren et al., 2012). For example, elevated tropospheric ozone (O_3) concentrations could reduce crop yields through direct or indirect influences on photosynthesis and stomatal conductance (Avnery et al., 2011; Booker et al., 2009; Farage et al., 1991; Martin et al., 2000; Pell et al., 1997; Tjoelker et al., 1995; Wittig et al., 2007). When combined with extreme climate conditions (e.g., heat and drought) or intensive management (i.e., excessive fertilizer application), O_3 pollution can substantially reduce the yield (Felzer et al., 2005; Ren et al., 2007, 2010; Tian,

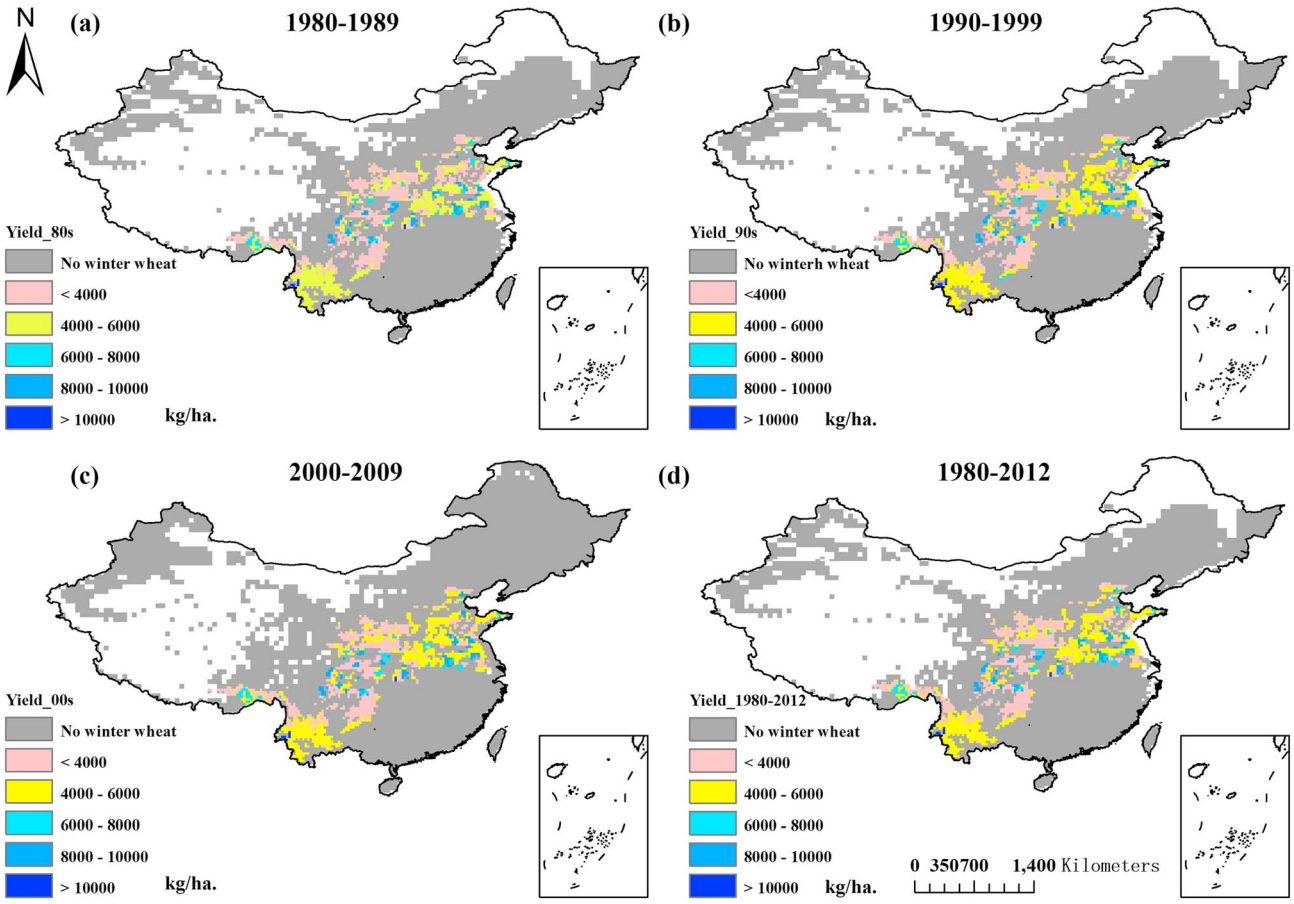

Figure 11. Spatial distribution of the DLEM-AG2.0-estimated winter wheat yield in China in the 1980s (a), the 1990s (b), the 2000s (c), and the study period 1980–2012 (d).

Ren, et al., 2016). For instance, simulated by the DLEM-Ag (a previous version), China's crop yield would have increased significantly (5% and 10%) if O_3 levels had been reduced (50% and 100%); spring wheat was the most sensitive to O_3, showing a reduction of 5.5% in extreme droughts and a reduction of 11.6% with extreme droughts with O_3 (Tian, Ren, et al., 2016). Therefore, the overall effects on crop production of multiple environmental stresses that interactively influence the photosynthesis process, the stomatal conductance, and nutrient/water conditions, etc., are complex. Here we compared our results under all-combined multifactor changes with the observations from 1980 to 2012 at both site and country levels. In general, the DLEM-AG2.0 simulations agreed well with the observations, with NRMSE of less than 20% for the simulations. To increase the estimation accuracy for the crop yield, addressing the interactive effect of multiple factors is clearly of critical importance.

4.2. Improvements of Crop Yield Simulation

Agriculture has serious effects on the terrestrial carbon cycle, and the consequences of agricultural management for carbon fluxes have been included only recently in earlier land surface modeling within the DLEM framework (Ren et al., 2011). Previous versions of the agricultural module in DLEM either presented a crude representation of crops or omitted many traits that are important, such as a process-based crop phenology and biomass allocation. DLEM-AG2.0, which is capable of simulating phenological development, leaf area growth, biomass allocation for different crop components (leaf, stem, root, and grain) at a daily time step, and the mechanism of crop development have been represented because of integrating interactive process-based crop models. For example, DLEM-Ag used MODIS LAI and substantial observation data to develop the phenology for each cropping system. The results of simulation are frequently limited by the quantity and quality of the data and might come with a significant amount of uncertainty. In DLEM-AG2.0,

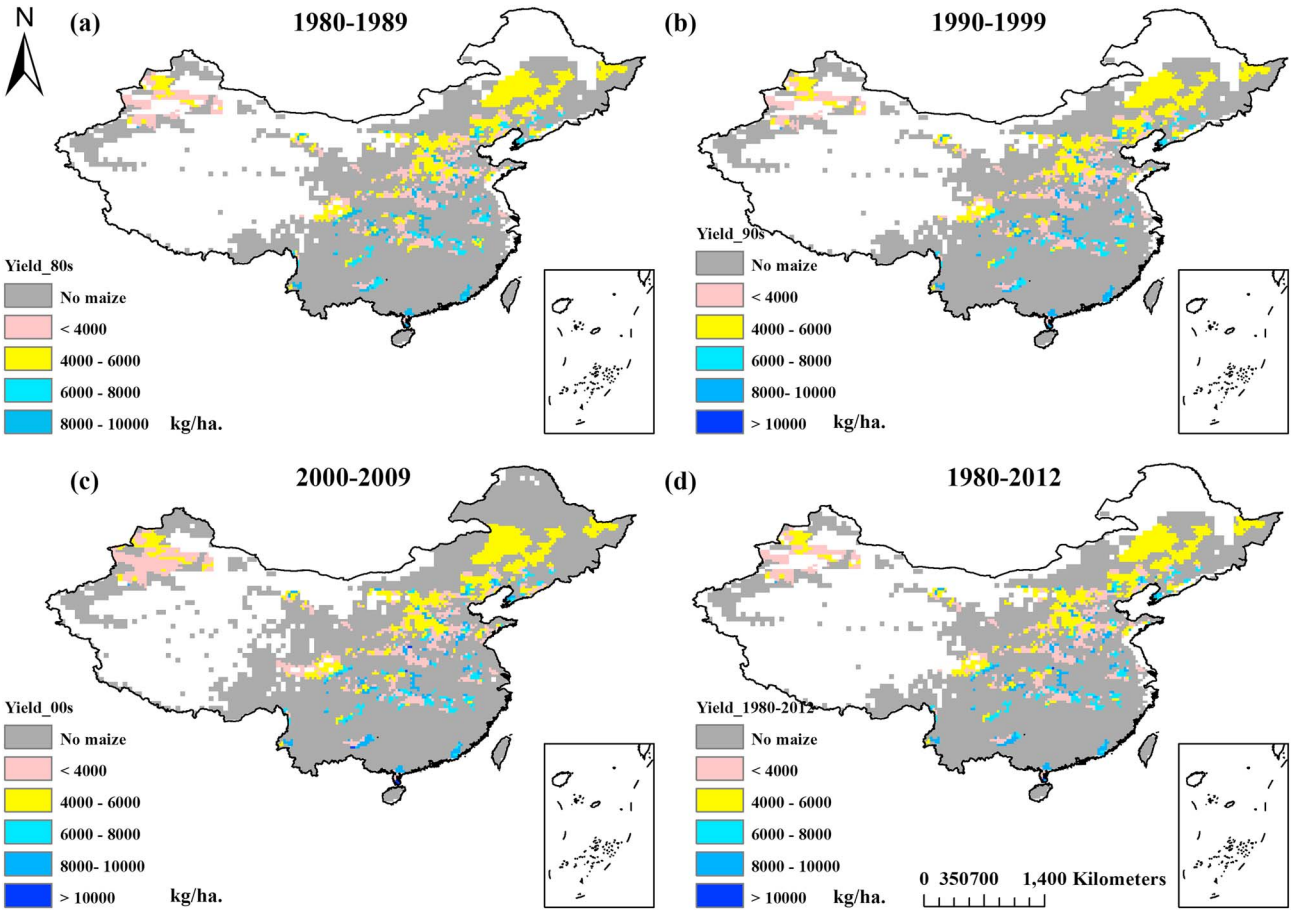

Figure 12. Spatial distribution of the DLEM-AG2.0 estimated maize yield in China in the 1980s (a), the 1990s (b), the 2000s (c), and the study period 1980–2012 (d).

the timing of each growth stage is determined by the ATT (°C day) adjusted by various impact factors, especially the critical temperature thresholds. At present, the impacts of minimum critical temperature threshold ($Card_{min}$) on crop production were represented in some atmosphere-land models (e.g., CLM-Crop) by GDD. However, the effect of the optimal ($Card_{opt}$) and maximum ($Card_{max}$) critical temperature thresholds on crop production is lacking in many models, which may bias the projection of climatic impacts. Temperature is one of the major environment factors affecting the growth, development, and yields of crops especially the rate of development. On one hand, crops have basic temperature requirements for completing a specific growth stage or the entire lifecycle. On the other hand, extremely high and low temperatures can have detrimental effects on crop growth, development, and yield, particularly at a critical growth stage such as anthesis (Asseng et al., 2011). Lobell et al. (2012) noted that when exposed to temperatures greater than 34 °C, wheat can experience desiccated pollen and increased kernel abortion during flowering, reducing the net photosynthesis rates, increasing vapor pressure deficit, and speeding up senescence. The effects of extreme temperature episodes close to the time of anthesis were more important to the yield of many crops than the effects of the increase in mean seasonal temperature of approximately 2 °C (Wheeler et al., 2000). Crops grow and develop ideally within the range of optimal temperature and at a slower rate beyond the range (Luo, 2011). Information on critical temperature thresholds for calculating crop growth stages can be used to improve crop models for accurate quantification of the impacts of temperature change on crop production at regional level.

Compared with the DLEM-Ag, another important improvement in the DLEM-AG2.0 was the integration of dynamic biomass allocation into the agricultural module. The DLEM-Ag estimated the crop yield simply through constant harvest index of each crop type (Ren et al., 2012). However, the harvest index is a location-specific and cultivar-specific parameter that is affected by crop variety, climate change, and other

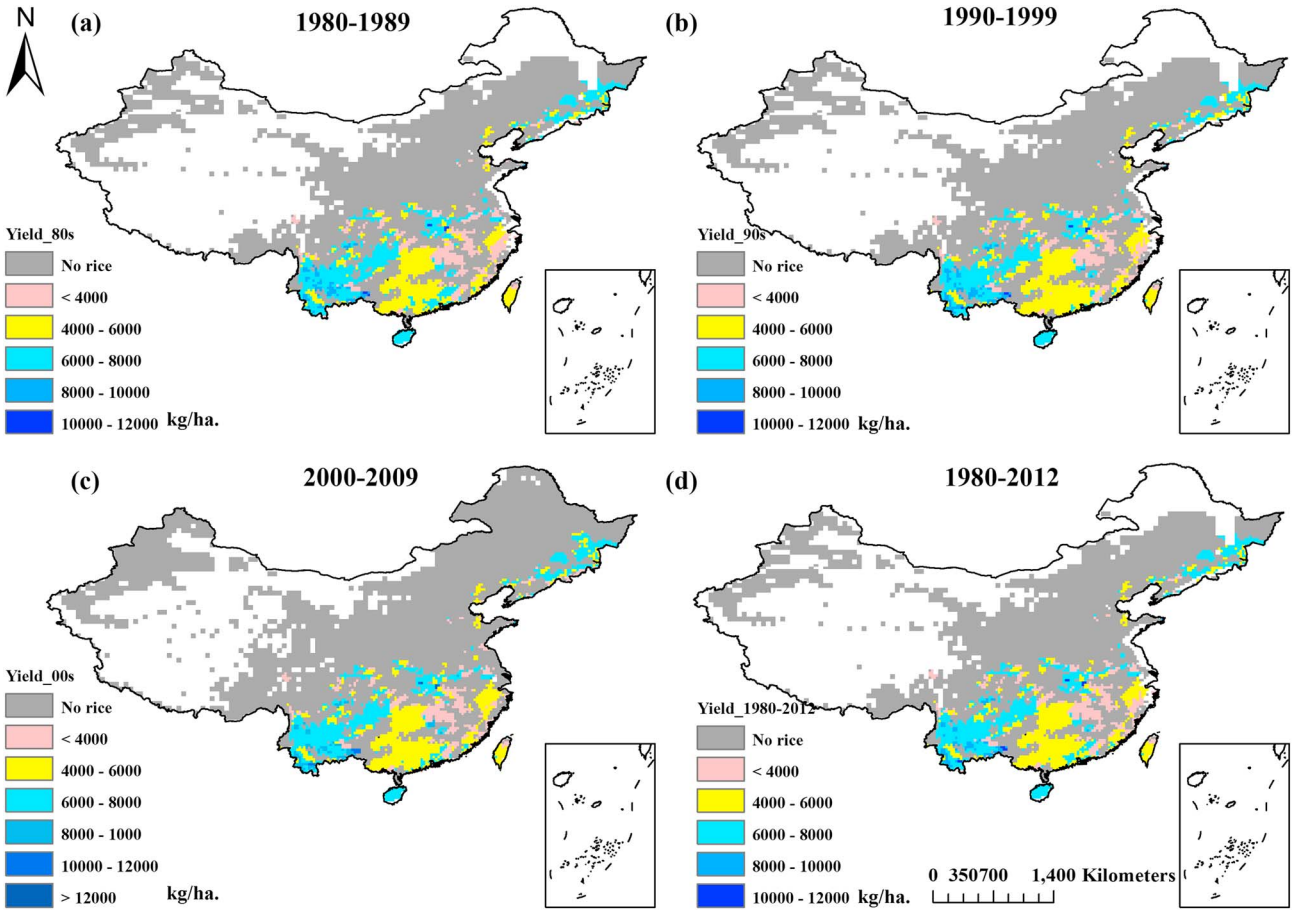

Figure 13. Spatial distribution of the DLEM-AG2.0 estimated rice yield in China in the 1980s (a), the 1990s (b), the 2000s (c), and the study period 1980–2012 (d).

environmental factors. For example, Prasad et al. (2006) indicated that the harvest index of rice would decrease significantly in response to high-temperature stress. The biomass allocation in DLEM-Ag2.0 is affected by allocation coefficients, light, water, nitrogen, critical temperature thresholds, and others, which optimize the mechanism and improve the accuracy of model simulations. Moreover, we could simulate the leaf, stem, and grain biomasses of each crop type, which would be conducive to further modifying DLEM-Ag2.0 and validating the accuracy of the simulation.

4.3. Uncertainties and Future Research Need

Our estimation of crop yield has some uncertainties resulting from the input data, model structure, and parameters. First, the DLEM-AG2.0 simulation needs a number of data sets that include climate, atmospheric chemical components, soil properties, land use and land cover, and agricultural management practices data. Many of the data used, while available at the national or global scale, still come with a significant amount of uncertainties. This requirement highlights the level of data needed to run the experiments in a representative way. Our goal was to expand the range of environmental factors to attempt to simulate a real ecological system. However, notably, some of the uncertainties associated with the individual data sets could limit the results. For example, because of limited data regarding O_3 concentrations throughout China, we used the modeled AOT_{40} values developed by Felzer et al. (2005) and Ren et al. (2007). Although the index has often been used to represent vegetation damage due to O_3, the accumulated hourly O_3 dose below a threshold of 40 p.p.b. in p.p.b./hr would be ignored and could limit the accuracy of the results. However, our photosynthesis module has the potential ability to incorporate O_3 concentrations as input if the O_3 flux data are available.

Second, the current DLEM-AG2.0 framework allows natural vegetation to change with time; meanwhile, managed croplands as they are treated in this model can expand or contract. We have incorporated the map of China's crop geographic distribution with regional agricultural census data derived from the Food and Agriculture Organization of the United Nations Statistics Division along with the multiple rotation types to generate the distribution of crop fields. However, discrepancies exist among the various crop distribution maps because the cultivation area ratio of a crop in a grid is less than 0.1 for some regions of the world. Moreover, we should recognize that the mechanisms acting in real ecological systems, especially for intensively managed agroecosystems, are very complicated. For example, other agricultural practices (e.g., tillage, residue management, and automatic planting date adjustment), natural disturbance (e.g., insect pests), and varieties distribution also affect crop carbon sequestration potential in croplands.

Third, we have set several different ATT targets for crop growth gained from field experiments, which are location-specific or cultivar-specific parameters. However, other studies have indicated that the validity of such values for regional simulation is questionable (e.g., Iizumi et al., 2014). Two opposite points of view exist about the ATT requirements of crops. One is that crop always requires the same amount of the ATT and depends only on the cultivar to reach a certain developmental stage (Sacks & Kucharik, 2011). The opposite view is that the ATT required for the completion of a given growth period of a particular cultivar is not constant but may vary with other environmental conditions (Liu, Hubbard, et al., 2013; Major et al., 1983). For example, Liu, Hubbard, et al. (2013) showed that for maize cultivar of ZD958, the ATT requirements during the vegetative growth period increased significantly, but the ATT requirements during the reproductive growth period decreased significantly with latitudes northward in China. Thus, even though we have calibrated the parameters to minimize the difference of yields between simulation and observation, the aggregation of parameters might be the major issue and increase the inaccuracy of the results. Next, we will improve the method of calculating ATT for crop development, considering longitude/latitude/elevation, bright sunshine hours, soil water stress, and others.

We also recognized that grain biomass is lower than the observations after the grain filling stage in our study, likely due to the missed reallocation processes in DLEM-AG2.0. In fact, if the supply in assimilation (daily biomasses increase) is insufficient to meet grain demand, then retranslocation may occur to meet the shortfall (Bouman et al., 2001; Keating et al., 2003; Mccown et al., 1996; Uehara & Tsuji, 1991). For example, from the start of grain filling, the wheat allows a total retranslocation of up to 20% of Stem biomasses per day (Mccown et al., 1996). Thus, as grain development relies on retranslocated biomass from the leaves and stems, the retranslocation scheme should be included in the next release of the DLEM-AG2.0.

Although the crop representation in the DLEM-AG2.0 is flexible for extrapolating to a global scale, rigorous testing is needed to ensure that crop behavior is consistent with regional observations. For example, our parameter calibration focused on crop species grown in China; expanding these parameters to capture other cultivars grown more broadly would improve the model's ability to capture global crop productivity. Uncertainty may also come from the inadequacy of the model representations. Currently, the DLEM-AG2.0 has not yet been coupled with the atmospheric circulation models with land processes and thus is unable to simulate the feedbacks between the crop growth and the climate system. Terrestrial ecosystem and climate system interact with each other through biophysics and biochemical processes that involve the transfers of energy, water, and other matters (Osborne et al., 2009). For example, LAI of the crop will give a feedback influence on climate change through biophysical responses to surface fluxes of greenhouse gases, albedo, and heat fluxes, which will lead to the changes of temperature, humidity, wind, and precipitation (Iizumi et al., 2014; Levis et al., 2012; Osborne et al., 2009). Several additional issues have been identified for advancing our research in the future, including (1) improving model temporal and spatial resolutions of input data because of the complicated cropping systems and land management practices in China, (2) improving reallocation processes for driving the model, (3) improving regional and global parameterization for main crop cultivars, and (4) improving the method of calculating ATT for crop development.

5. Conclusion

In this work, the DLEM-AG2.0, a new version of the DLEM Agricultural module, has been developed for better simulation of the dynamic processes of crop growth and development at a daily time step, while including growth period development, biomass accumulation, biomass allocation, and yield formation. In addition to

making comparisons to previous studies, this work addressed how crop yield has been affected by multifactor environmental changes, including climate change, CO_2 concentration, tropospheric O_3, nitrogen deposition, land use/cover change, N fertilizer, and irrigation. A comparison of simulated crop yield for wheat, maize, and rice with the measured and survey data at both site and country levels during 1980–2012 revealed that the DLEM-AG2.0 simulations agreed well with the observations with the NRMSE of the simulations less than 20%. Rigorous validation with both site-specific and regional observations is necessary for a global application of the agricultural module. Further advancement of agricultural modeling within the Earth system modeling framework will require consideration of human perception and behavior for adapting and mitigating global change.

Acknowledgments

This study has been supported by the National Key R & D Program of China (no. 2018YFA0606001), the US National Science Foundation (1210360, 1243232), the Chinese Academy of Sciences STS Program (KFJ-STS-ZDTP-0), SKLURE Grant (SKLURE2017-1-6), and the OUC-AU Joint Center Grant Program. We thank Wei Ren, Mingliang Liu, Chaoqun Lu, Guangsheng Chen, and other previous DLEM developers for their contribution. The model input and output data in this study are archived in the International Center for Climate and Global Change Research at Auburn University (http://wp.auburn.edu/cgc/).

References

Amanullah, M. J. H., Nawab, K., & Ali, A. (2007). Response of specific leaf area (SLA), leaf area index (LAI) and leaf area ratio (LAR) of maize (*Zea mays* L.) to plant density, rate and timing of nitrogen application. *World Applied Sciences Journal*, *2*, 235–243.

Asseng, S., Foster, I., & Turner, N. C. (2011). The impact of temperature variability on wheat yields. *Global Change Biology*, *17*(2), 997–1012.

Asseng, S., Keating, B. A., Fillery, I. R. P., Gregory, P. J., Bowden, J. W., Turner, N. C., et al. (1998). Performance of the APSIM-wheat model in Western Australia. *Field Crops Research*, *57*(2), 163–179.

Aunan, K., Berntsen, T. K., & Seip, H. M. (2000). Surface ozone in China and its possible impact on agriculture crop yields. *Ambio*, *29*, 294–301.

Avnery, S., Mauzerall, D. L., Liu, J. F., & Horowitz, L. W. (2011). Global crop yield reductions due to surface ozone exposure: 1. Year 2000 crop production losses and economic damage. *Atmospheric Environment*, *45*, 2284–2296.

Awal, M. A., Koshi, H., & Ikeda, T. (2005). Radiation interception and use by maize/peanut intercrop canopy. *Agricultural and Forest Meteorology*, *139*, 74–83.

Bernacchi, C. J., Singsaas, E. L., Pimentel, C., Portis, A. R., & Long, S. P. (2001). Improved temperature response functions for models of Rubisco-limited photosynthesis. *Plant, Cell & Environment*, *24*(2), 253–259.

Bonan, G. B. (1996). Land surface model (LSM version 1.0) for ecological, hydrological, and atmospheric studies: Technical description and user's guide. Technical note. National Center for Atmospheric Research, Boulder, CO (United States). Climate and Global Dynamics Div.

Bondeau, A., Smith, P. C., Zaehle, S., Schaphoff, S., Lucht, W., Cramer, W., et al. (2007). Modelling the role of agriculture for the 20th century global terrestrial carbon balance. *Global Change Biology*, *13*(3), 679–706. https://doi.org/10.1111/j.1365-2486.2006.01305.x

Booker, F., Muntifering, R., McGrath, M., Burkey, K., Decoteau, D., Fiscus, E., et al. (2009). The ozone component of global change: Potential effects on agricultural and horticultural plant yield, product quality and interactions with invasive species. *Journal of Integrative Plant Biology*, *51*, 337–351.

Boonjung, H., & Fukai, S. (1996). Effects of soil water deficit at different growth stages on rice growth and yield under upland conditions. 2. Phenology, biomass production and yield. *Field Crops Research*, *48*(1), 47–55.

Borlaug, N. (2007). Feeding a hungry world. *Science*, *318*(5849), 359. https://doi.org/10.1126/science.1151062

Bouman, B. A. M., Kroppff, M. J., Tuong, T. P., Wopereis, M. C. S., Ten Berge, H. F. M., & van Laar, H. H. (2001). *ORYZA2000: modeling lowland rice*, (pp. 1–158). Los Banos: International Rice Research Institute.

Cai, Y., Ding, W., & Luo, J. (2013). Nitrous oxide emission from Chinese maize-wheat rotation systems: A 3-year field measurement. *Atmospheric Environment*, *65*, 112–122.

Calderini, D. F., Dreccer, M. F., & Slafer, G. A. (1997). Consequences of breeding on biomass, radiation interception and radiation-use efficiency in wheat. *Field Crops Research*, *52*, 271–281.

Chen, C., Lawes, R., Fletcher, A., Oliver, Y., Robertson, M., Bell, M., & Wang, E. (2016). How well can APSIM simulate nitrogen uptake and nitrogen fixation of legume crops? *Field Crops Research*, *187*, 35–48.

Chen, C., Wang, E., & Yu, Q. (2010a). Modelling the effects of climate variability and water management on crop water productivity and water balance in the North China Plain. *Agricultural Water Management*, *97*(8), 1175–1184.

Chen, C., Wang, E., & Yu, Q. (2010b). Modeling wheat and maize productivity as affected by climate variation and irrigation supply in North China Plain. *Agronomy Journal*, *102*(3), 1037–1049.

Cole, C. V., Williams, J., Shaffer, M., & Hanson, J. (1987). Nutrient and organic matter dynamics as components of agricultural production systems models. In *Soil fertility and organic matter as critical components of production system*, *SSSA Spec. Pub.*, (Vol. 19, pp. 147–166). Madison, WI: Soil Science Society of America and American Society of Agronomy.

Collatz, G. J., Ball, J. T., Grivet, C., & Berry, J. A. (1991). Physiological and environmental regulation of stomatal conductance, photosynthesis and transpiration: A model that includes a laminar boundary layer. *Agricultural and Forest Meteorology*, *54*(2–4), 107–136.

Cook, B. I., Shukla, S. P., Puma, M. J., & Nazarenko, L. S. (2014). Irrigation as an historical climate forcing. *Climate Dynamics*, *44*, 1715. https://doi.org/10.1007/s00382-014-2204-7

Cui, F., Yan, G., Zhou, Z., Zheng, X., & Deng, J. (2012). Annual emissions of nitrous oxide and nitric oxide from a wheat-maize cropping system on a silt loam calcareous soil in the North China Plain. *Soil Biology & Biochemistry*, *48*(4), 10–19.

Detmann, K. C., Araujo, W. L., Martins, S. C., Sanglard, L. M. V. P., Reis, J. V., Detmann, E., et al. (2012). Silicon nutrition increases grain yield, which, in turn, exerts a feed-forward stimulation of photosynthetic rates via enhanced mesophyll conductance and alters primary metabolism in rice. *New Phytologist*, *196*, 752–762.

Diffenbaugh, N. S. (2009). Influence of modern land cover on the climate of the United States. *Climate Dynamics*, *33*, 945–958.

Ding, Y. J., Ye, B. S., Han, T. D., Shen, Y. P., & Liu, S. Y. (2007). Regional difference of annual precipitation and discharge variation over west China during the last 50 years. *Science China Earth Sciences*, *50*(6), 936–945.

Dingkuhn, M., Johnson, D. E., Sow, A., & Audebert, A. Y. (1999). Relationships between upland rice canopy characteristics and weed competitiveness. *Field Crops Research*, *61*, 79–95.

Dong, W., Chen, J., Zhang, B., Tian, Y., & Zhang, W. (2011). Responses of biomass growth and grain yield of midseason rice to the anticipated warming with FATI facility in East China. *Fuel and Energy Abstracts*, *123*(3), 259–265.

Drewniak, B., Song, J., Prell, J., Kotamarthi, V. R., & Jacob, R. (2013). Modeling agriculture in the Community Land Model. *Geoscientific Model Development*, *6*(2), 495–515.

Evans, J. R., & Poorter, H. (2001). Photosynthetic acclimation of plants to growth irradiance: The relative importance of specific leaf area and nitrogen partitioning in maximizing carbon gain. *Plant, Cell & Environment*, *24*(8), 755–767.
Food and Agriculture Organization (2017). FAOSTAT database. Retrieved from http://www.fao.org/faostat/en/#data/TP/visualize
Farage, P. K., Long, S. P., Lechner, E. G., & Baker, N. R. (1991). The sequence of change within the photosynthetic apparatus of wheat following short-term exposure to ozone. *Plant Physiology*, *95*, 529–535.
Farquhar, G. D., Camerer, S. V., & Berry, J. A. (1980). A biochemical-model of photosynthetic CO_2 assimilation in leaves of C3 species. *Planta*, *149*, 78–90.
Felzer, B. S., Kicklighter, D. W., Melillo, J. M., Wang, C., Zhuang, Q., & Prinn, R. (2004). Effects of ozone on net primary production and carbon sequestration in the conterminous United States using a biogeochemistry model. *Tellus*, *56B*, 230–248.
Felzer, B., Reilly, J., Melillo, J., Kicklighter, D., Sarofim, M., Wang, C., et al. (2005). Future effects of ozone on carbon sequestration and climate change policy using a global biogeochemical model. *Climatic Change*, *73*, 345–373.
Feng, L. P., Bouman, B. A. M., Tuong, T. P., Cabangon, R. J., Li, Y. L., Lu, G. A., & Feng, Y. H. (2007). Exploring options to grow rice using less water in northern China using a modelling approach: I. Field experiments and model evaluation. *Agricultural Water Management*, *88*(1–3), 1–13.
Flénet, F., Kiniry, J. R., Board, J. E., Westgate, M. E., & Reicosky, D. C. (1996). Row spacing effects on light extinction coefficients of corn, sorghum, soybean, and sunflower. *Agronomy Journal*, *88*, 185–190.
Gifford, G. M. (1995). Whole plant respiration and photosynthesis of wheat under increased CO_2 concentration and temperature: Long-term vs. short-term distinctions for modelling. *Global Change Biology*, *1*(6), 385–396. https://doi.org/10.1111/j.1365-2486.1995.tb00037.x
Goldewijk, K. K., Beusen, A., van Drecht, G., & de Vos, M. (2011). The HYDE 3.1 spatially explicit database of human-induced global land-use change over the past 12,000 years. *Global Ecology and Biogeography*, *20*(1), 73–86.
Gomez, K. A., & Gomez, A. A. (1984). *Statistical procedures for agricultural research*, (2nd ed.p. 680). New York: John Wiley.
Guimberteau, M., Laval, K., Perrier, A., & Polcher, J. (2012). Global effect of irrigation and its impact on the onset of the Indian summer monsoon. *Climate Dynamics*, *39*(6), 1329–1348. https://doi.org/10.1007/s00382-011-1252-5
Han, X. L., Jing, Y. S., Hao, Y., & Geng, L. N. (2013). The comparison of regional parameters of ORYZA2000 based on the field test. *Journal of Arid Meteorology*, *31*(1), 37–42.
Holland, E. A., Braswell, B. H., Lamarque, J. F., Townsend, A., Sulzman, J., Müller, J. F., et al. (1997). Variations in the predicted spatial distribution of atmospheric nitrogen deposition and their impact on carbon uptake by terrestrial ecosystems. *Journal of Geophysical Research*, *102*, 15,849–15,866.
Holzworth, D. P., Huth, N. I., Devoil, P. G., Zurcher, E. J., Herrmann, N. I., McLean, G., et al. (2014). APSIM – Evolution towards a new generation of agricultural systems simulation. *Environmental Modelling & Software*, *62*(C), 327–350.
Hu, F., Gan, Y., Cui, H., Zhao, C., Feng, F., Yin, W., & Chai, Q. (2016). Intercropping maize and wheat with conservation agriculture principles improves water harvesting and reduces carbon emissions in dry areas. *European Journal of Agronomy*, *74*, 9–17.
Hund, A., Frascaroli, E., Leipner, J., Jompuk, C., Stamp, P., & Fracheboud, Y. (2005). *Molecular Breeding*, *16*, 321.
Hurtt, G. C., Frolking, S., Fearon, M. G., Moore, B., Shevliakova, E., Malyshev, S., et al. (2006). The underpinnings of land-use history: Three centuries of global gridded land-use transitions, wood harvest activity, and resulting secondary lands. *Global Change Biology*, *12*, 1208–1229.
Iizumi, T., Tanaka, Y., Sakurai, G., Ishigooka, Y., & Yokozawa, M. (2014). Dependency of parameter values of a crop model on the spatial scale of simulation. *Journal of Advances in Modeling Earth Systems*, *6*(3), 527–540.
Jamieson, P. D., Porter, J. R., & Wilson, D. R. (1991). A test of the computer simulation model ARCWHEAT1 on wheat crops grown in New Zealand. *Field Crops Research*, *27*, 337–350.
Jing, Q., Bouman, B. A. M., Hengsdijk, H., van Keulen, H., & Cao, W. (2007). Exploring options to combine high yields with high nitrogen use efficiencies in irrigated rice in China. *European Journal of Agronomy*, *26*(2), 166–177.
Jone, J. W., Hoogenboom, G., Porter, C. H., Boote, K. J., Batchelor, W. D., Hunt, L. A., et al. (2003). The DSSAT cropping system model. *European Journal of Agronomy*, *18*, 235–265.
Jones, C. A., & Kiniry, J. R. (1986). *CERES-Maize: A simulation model of maize growth and development*, (p. 194). College Station, TX: Texas A&M Univ. Press.
Keating, B. A., Carberry, P. S., Hammer, G. L. M. E., Probert, M. J., Robertson, D., Holzworth, N. I., et al. (2003). An overview of APSIM, a model designed for farming systems simulation. *European Journal of Agronomy*, *18*(3–4), 267–288.
Kucharik, C. J. (2003). Evaluation of a process-based agroecosystem model (Agro-IBIS) across the U.S. corn belt: Simulations of the interannual variability in maize yield. *Earth Interactions*, *7*, 7–14.
Leff, B., Ramankutty, N., & Foley, J. A. (2004). Geographic distribution of major crops across the world. *Global Biogeochemical Cycles*, *18*, GB1009. https://doi.org/10.1029/2003GB002108
Leng, G., Zhang, X., Huang, M., Yang, Q., Rafique, R., Asrar, G. R., & Ruby Leung, L. (2016). Simulating county-level crop yields in the conterminous United States using the community land model: The effects of optimizing irrigation and fertilization. *Journal of Advances in Modeling Earth Systems*, *8*, 1912–1931. https://doi.org/10.1002/2016MS000645
Levis, S., Gordon, B. B., Erik Kluzek, P. E., Thornton, A., Jones, W. J. S., & Kucharik, C. J. (2012). Interactive Crop Management in the Community Earth System Model (CESM1): Seasonal influences on land-atmosphere fluxes. *Journal of Climate*, *25*(14), 4839–4859. https://doi.org/10.1175/JCLI-D-11-00446.1
Li, Y. L., Cui, J. Y., Zhang, T. H., & Zhao, H. L. (2003). Measurement of evapotranspiration of irrigated spring wheat and maize in a semi-arid region of North China. *Agricultural Water Management*, *61*(1), 1–12.
Liu, B., Liu, L. L., Asseng, S., Zou, X. D., Li, J., Cao, W. X., & Zhu, Y. (2016). Modelling the effects of heat stress on post-heading durations in wheat: A comparison of temperature response routines. *Agricultural and Forest Meteorology*, *222*, 45–58.
Liu, C., Wang, K., Meng, S., Zheng, X., Zhou, Z., Han, S., et al. (2011). Effects of irrigation, fertilization and crop straw management on nitrous oxide and nitric oxide emissions from a wheat-maize rotation field in northern China. *Agriculture Ecosystems & Environment*, *140*(1–2), 226–233.
Liu, J., Shen, J., Li, Y., Su, Y., Ge, T., Jones, D. L., & Wu, J. (2014). Effects of biochar amendment on the net greenhouse gas emission and greenhouse gas intensity in a Chinese double rice cropping system. *European Journal of Soil Biology*, *65*, 30–39.
Liu, M., Tian, H., Yang, Q., Yang, J., Song, X., Lohrenz, S. E., & Cai, W. J. (2013). Long-term trends in evapotranspiration and runoff over the drainage basins of the Gulf of Mexico during 1901–2008. *Water Resources Research*, *49*, 1988–2012.
Liu, M. L., & Tian, H. Q. (2010). China's land-cover and land-use change from 1700 to 2005: Estimations from high-resolution satellite data and historical archives. *Global Biogeochemical Cycles*, *24*, GB3003. https://doi.org/10.1029/2009GB003687
Liu, M. L., Tian, H. Q., Chen, G. S., Ren, W., Zhang, C., & Liu, J. (2008). Effects of land use and land cover change on evapotranspiration and water yield in China during the 20th century. *Journal of the American Water Resources Association*, *44*(5), 1193–1207.

Liu, S., Zhang, L., Liu, Q., & Zou, J. (2012). Fe (III) fertilization mitigating net global warming potential and greenhouse gas intensity in paddy rice-wheat rotation systems in China. *Environmental Pollution*, *164*(9), 73–80.

Liu, X. Y., Qu, J. J., Li, L. Q., Zhang, A. F., Jufeng, Z., Zheng, J. W., & Pan, G. X. (2012). Can biochar amendment be an ecological engineering technology to depress N_2O emission in rice paddies—A cross site field experiment from southern China. *Ecological Engineering*, *42*(9), 168–173.

Liu, Y., Zhou, Z., Zhang, X., Xu, X., Chen, H., & Xiong, Z. (2015). Net global warming potential and greenhouse gas intensity from the double rice system with integrated soil-crop system management: A three-year field study. *Atmospheric Environment*, *116*, 92–101.

Liu, Y. T., Li, Y. E., Wan, Y. F., Chen, D. L., Gao, Q. Z., Li, Y., & Qin, X. B. (2011). Nitrous oxide emissions from irrigated and fertilized spring maize in semi-arid northern China. *Agriculture Ecosystems & Environment*, *141*(3–4), 287–295.

Liu, Y. Y., Evans, J. P., McCabe, M. F., de Jeu, R. A., van Dijk, A. I., Dolman, A. J., & Saizen, I. (2013). Changing climate and overgrazing are decimating Mongolian steppes. *PLoS ONE*, *8*, e57599.

Liu, Z. J., Hubbard, K. G., Lin, X. M., & Yang, X. G. (2013). Negative effects of climate warming on maize yield are reversed by the changing of sowing date and cultivar selection in Northeast China. *Global Change Biology*, *19*(11), 3481–3492.

Loague, K., & Green, R. E. (1991). Statistical and graphical methods for evaluating solute transport models: Overview and application. *Journal of Contaminant Hydrology*, *7*, 51–73. https://doi.org/10.1016/0169-7722(91)90038-3

Lobell, D. B., Bala, G., Bonfils, C., & Duffy, P. B. (2006). Potential bias of model projected greenhouse warming in irrigated regions. *Geophysical Research Letters*, *33*, L13709. https://doi.org/10.1029/2006GL026770

Lobell, D. B., & Field, C. B. (2007). Global scale climate-crop yield relationships and the impacts of recent warming. *Environmental Research Letters*, *2*, 014002. https://doi.org/10.1088/1748-9326/2/1/014002

Lobell, D. B., Sibley, A., & Ortiz-Monasterio, J. I. (2012). Extreme heat effects on wheat senescence in India. *Nature Climate Change*, *29*, 196–189.

Lu, C. Q., & Tian, H. Q. (2007). Spatial and temporal patterns of nitrogen deposition in China: Synthesis of observational data. *Journal of Geophysical Research*, *112*, D22S05. https://doi.org/10.1029/2006JD007990

Lu, C. Q., & Tian, H. Q. (2013). Net greenhouse gas balance in response to nitrogen enrichment: Perspectives from a coupled biogeochemical model. *Global Change Biology*, *19*(2), 571–588. https://doi.org/10.1111/gcb.12049

Lu, C. Q., Tian, H. Q., Liu, M., Ren, W., Xu, X., Chen, G., & Zhang, C. (2012). Effect of nitrogen deposition on China's terrestrial carbon uptake in the context of multi-factor environmental changes. *Ecological Applications*, *22*, 53–75.

Lunagaria, M. M., & Shekh, A. M. (2006). Radiation interception, light extinction coefficient and leaf area index of wheat (*Triticum aestivum* L.) crop as influenced by row orientation and row spacing. *The Journal of Agricultural Science*, *2*, 43–54.

Luo, Q. Y. (2011). Temperature thresholds and crop production: A review. *Climatic Change*, *109*(3–4), 563–598.

Ma, Y. C., Kong, X. W., Yang, B., Zhang, X. L., Yan, X. Y., Yang, J. C., & Xiong, Z. Q. (2013). Net global warming potential and greenhouse gas intensity of annual rice-wheat rotations with integrated soil-crop system management. *Agriculture Ecosystems & Environment*, *164*(1), 209–219.

Magill, A. H., Aber, J. D., Berntson, G. M., McDowell, W. H., Nadelhoffer, K. J., Melillo, J. M., & Steudler, P. (2000). Long-term nitrogen additions and nitrogen saturation in two temperate forests. *Ecosystems*, *3*, 238–253.

Major, D. J., Brown, D. M., Bootsma, A., Dupuis, G., Fairey, N. A., Grant, E. A., et al. (1983). An evaluation of the corn heat unit system for the short-season growing regions across Canada. *Canadian Journal of Plant Science*, *63*, 121–130.

Martin, M. J., Farage, P. K., Humphries, S. W., & Long, S. P. (2000). Can the stomatal changes caused by acute ozone exposure be predicted by changes occurring in the mesophyll? A simplification for models of vegetation response to the global increase in tropospheric elevated ozone episodes. *Australian Journal of Plant Physiology*, *27*, 211–219.

Matson, P., Lohse, K. A., & Hall, S. J. (2002). The globalization of nitrogen deposition: Consequences for terrestrial ecosystems. *Ambio*, *31*, 113–119.

Mccown, R. L., Hammer, G. L., Hargreaves, J. N. G., Holzworth, D. P., & Freebairn, D. M. (1996). APSIM: A novel software system for model development, model testing and simulation in agricultural systems research. *Agricultural Systems*, *50*(3), 255–271.

McDermid, S. S., Mearns, L. O., & Ruane, A. C. (2017). Representing agriculture in Earth system models: Approaches and priorities for development. *Journal of Advances in Modeling Earth Systems*, *9*, 2230–2265. https://doi.org/10.1002/2016MS000749

McMaster, G. G., White, J. W., Hunt, L. A., Jamieson, P. D., Dhillon, S. S., & Ortiz-Monasterio, J. I. (2008). Simulating the influence of vernalization, photoperiod and optimum temperature on wheat developmental rates. *Annals of Botany*, *102*(4), 561–569.

Mo, X., Liu, S., & Lin, Z. (2012). Evaluation of an ecosystem model for a wheat–maize double cropping system over the Northern China Plain. *Environmental Modelling & Software*, *32*(32), 61–73.

Mo, Z. H., Feng, L. P., Zou, H. P., Wang, J., Huang, W. H., & Yang, X. G. (2011). Validation and adaptability evaluation of rice growth model ORYZA2000 in double cropping rice area of Hunan Province. *Acta Ecologica Sinica*, *31*(16), 4628–4637.

Mohanty, M., Probert, M. E., Reddy, K. S., Dalal, R. C., Mishra, A. K., Subba Rao, A., et al. (2012). Simulating soybean–wheat cropping system: APSIM model parameterization and validation. *Agriculture Ecosystems & Environment*, *152*(15), 68–78.

Monfreda, C., Ramankutty, N., & Foley, J. A. (2008). Farming the planet: 2. Geographic distribution of crop areas, yields, physiological types, and net primary production in the year 2000. *Global Biogeochemical Cycles*, *22*, GB1022. https://doi.org/10.1029/2007GB002947

Neff, J. C., Hobbie, S. E., & Vitousek, P. M. (2000). Nutrient and mineralogical control on dissolved organic C, N and P fluxes and stoichiometry in Hawaiian soils. *Biogeochemistry*, *51*, 283–302.

Neitsch, S. L., Arnold, J. G., Kiniry, J. R., & Williams, J. R. (2005). *Soil and water assessment tool, theoretical documentation: Version 2005*. Temple, TX: USDA Agricultural Research Service and Texas A&M Blackland Research Center.

Ollinger, S. V., Aber, J. D., & Reich, P. B. (1997). Simulating ozone effects on forest productivity: Interactions among leaf-canopy and stand-level processes. *Ecological Applications*, *7*, 1237–1251.

Okada, M., Iizumi, T., Sakurai, G., Hanasaki, N., Sakai, T., Okamoto, K., & Yokozawa, M. (2015). Modeling irrigation-based climate change adaptation in agriculture: Model development and evaluation in Northeast China. *Journal of Advances in Modeling Earth Systems*, *7*, 1409–1424. https://doi.org/10.1002/2014MS000402

Osborne, T., Slingo, J., Lawrence, D., & Wheeler, T. (2009). Examining the interaction of growing crops with local climate using a coupled crop-climate model. *Journal of Climate*, *22*(6), 1393–1411. https://doi.org/10.1175/2008JCLI2494.1

Osborne, T. M., Lawrence, D. M., Challinor, A. J., Slingo, J. M., & Wheeler, T. R. (2006). Development and assessment of a coupled crop-climate model. *Global Change Biology*, *13*, 169–183. https://doi.org/10.1111/j.1365-2486.2006.01274.x

Pan, S., Tian, H., Dangal, S. R., Ouyang, Z., Lu, C., Yang, J., et al. (2015). Impacts of climate variability and extremes on global net primary production in the first decade of the 21st century. *Journal of Geographical Sciences*, *25*, 1027–1044.

Pan, S., Tian, H., Dangal, S. R., Zhang, C., Yang, J., Tao, B., et al. (2014). Complex spatiotemporal responses of global terrestrial primary production to climate change and increasing atmospheric CO_2 in the 21st century. *PLoS ONE*, *9*, e112810.
Pell, E. J., Schlagnhaufer, C. D., & Arteca, R. N. (1997). Ozone-induced oxidative stress: Mechanisms of action and reaction. *Physiologia Plantarum*, *100*, 264–273.
Pitman, A. J., de Noblet-Ducoudré, N., Cruz, F. T., Davin, E. L., Bonan, G. B., Brovkin, V., et al. (2009). Uncertainties in climate responses to past land cover change: First results from the LUCID intercomparison study. *Geophysical Research Letters*, *36*, L14814. https://doi.org/10.1029/2009GL039076
Porter, J. R., & Gawith, M. (1999). Temperatures and the growth and development of wheat: A review. *European Journal of Agronomy*, *10*, 23–36.
Potter, P., Ramankutty, N., Bennett, E. M., & Donner, S. D. (2010). Characterizing the spatial patterns of global fertilizer application and manure production. *Earth Interactions*, *14*, 1–22. https://doi.org/10.1175/2009EI288.1
Prasad, P. V. V., Boote, K. J., Allen, L. H. Jr., Sheehy, J. E., & Thomas, J. M. G. (2006). Species, ecotype and cultivar differences in spikelet fertility and harvest index of rice in response to high temperature stress. *Field Crops Research*, *95*(2–3), 398–411.
Reich, P. B. (1987). Quantifying plant response to ozone: A unifying theory. *Tree Physiology*, *3*, 63–91.
Rastetter, E. B., Agren, G. I., & Shaver, G. R. (1997). Responses of N-limited ecosystems to increased CO_2: A balanced-nutrition, coupled-element-cycles model. *Ecological Applications*, *7*, 444–460.
Rebetzke, G. J., Botwright, T. L., Moore, C. S., Richards, R. A., & Condon, A. G. (2004). Genotypic variation in specific leaf area for genetic improvement of early vigour in wheat. *Field Crops Research*, *88*(2–3), 179–189.
Ren, W., Tian, H., Liu, M., Zhang, C., Chen, G. S., Pan, S. F., et al. (2007). Effects of tropospheric ozone pollution on net primary productivity and carbon storage in terrestrial ecosystems of China. *Journal of Geophysical Research*, *112*, D22S09. https://doi.org/10.1029/2007JD008521
Ren, W., Tian, H. Q., Tao, B., Chappelka, A., Sun, G., Lu, C. W., et al. (2010). Impacts of tropospheric ozone and climate change on net primary productivity and net carbon exchange of China's forest ecosystems. *Global Ecology and Biogeography*, *20*(3), 391–406.
Ren, W., Tian, H. Q., Tao, B., Huang, Y., & Pan, S. (2012). China's crop productivity and soil carbon storage as influenced by multifactor global change. *Global Change Biology*, *18*, 2945–2957.
Ren, W., Tian, H. Q., Xu, X. F., Liu, M. L., Lu, C. Q., Chen, G. S., et al. (2011). Spatial and temporal patterns of CO_2 and CH_4 fluxes in China's croplands in response to multifactor environmental changes. *Tellus*, *63*(2), 222–240.
Ryan, M. G. (1991). Effects of climate change on plant respiration. *Ecological Applications*, *1*, 157–167.
Sacks, W. J., Deryng, D., Foley, J. A., & Ramankutty, N. (2010). Crop planting dates: An analysis of global patterns. *Global Ecology and Biogeography*, *19*, 607–620. https://doi.org/10.1111/j.1466-8238.2010.00551.x
Sacks, W. J., & Kucharik, C. J. (2011). Crop management and phenology trends in the U.S. Corn Belt: Impacts on yields, evapotranspiration and energy balance. *Agricultural and Forest Meteorology*, *151*, 882–894.
Saleque, M. A., Abedin, M. J., Bhuiyan, N. I., Zaman, S. K., & Panaullah, G. M. (2004). Long-term effects of inorganic and organic fertilizer sources on yield and nutrient accumulation of lowland rice. *Field Crops Research*, *86*(1), 53–65.
Sanchez, B., Rasmussen, A., & Porter, J. R. (2014). Temperatures and the growth and development of maize and rice: A review. *Global Change Biology*, *20*, 408–417.
Saxton, K., & Rawls, W. (2006). Soil water characteristic estimates by texture and organic matter for hydrologic solutions. *Soil Science Society of America Journal*, *70*, 1569–1578. https://doi.org/10.2136/sssaj2005.0117
Schindler, D. W. (2001). The cumulative effects of climate warming and other human stresses on Canadian freshwaters in the new millennium. *Canadian Journal of Fisheries and Aquatic Sciences*, *58*, 18–29.
Schindler, D. W., & Bayley, S. E. (1993). The biosphere as an increasing sink for atmospheric carbon—Estimates from increased nitrogen deposition. *Global Biogeochemical Cycles*, *7*, 717–733.
Sellers, P., Randall, D., Collatz, G., Berry, J., Field, C., et al. (1996). A revised land surface parameterization (SiB2) for atmospheric GCMs. Part I: Model formulation. *Journal of Climate*, *9*, 676–705.
Sharkey, T. D. (2005). Effects of moderate heat stress on photosynthesis: Importance of thylakoid reactions, Rubisco deactivation, reactive oxygen species, and thermotolerance provided by isoprene. *Plant, Cell and Environment*, *28*, 269–277. https://doi.org/10.1111/j.1365-3040.2005.01324.x
Shearman, V. J., Sylvester-Bradley, R., Scott, R. K., & Foulkes, M. J. (2005). Physiological processes associated with wheat yield progress in the UK. *Crop Science*, *45*, 175–185.
Smith, P. C., De Noblet-Ducoudre´, N., Ciais, P., Peylin, P., Viovy, N., Meurdesoif, Y., & Bondeau, A. (2010). European-wide simulations of croplands using an improved terrestrial biosphere model: Phenology and productivity. *Journal of Geophysical Research*, *115*, G01014. https://doi.org/10.1029/2008JG000800
Song, C. C., Wang, L. L., Tian, H. Q., Liu, D. Y., Lu, C. Q., Xu, X. F., et al. (2013). Effect of continued nitrogen enrichment on greenhouse gas emissions from a wetland ecosystem in the Sanjiang Plain, Northeast China: A 5 year nitrogen addition experiment. *Journal of Geophysical Research: Biogeosciences*, *118*, 741–751. https://doi.org/10.1002/jgrg.20063
Steduto, P., Hsiao, T. C., Raes, D., & Fereres, E. (2009). AquaCrop—The FAO crop model to simulate yield response to water: I. Concepts and underlying principles. *Agronomy Journal*, *101*, 426–437.
Sun, H. Y., Zhang, X. Y., Wang, E. L., Chen, S. Y., Shao, L. W., & Qin, W. L. (2016). Assessing the contribution of weather and management to the annual yield variation of summer maize using APSIM in the North China Plain. *Field Crops Research*, *194*, 94–102.
Swarup, A., & Singh, K. N. (1989). Effect of 12 years' rice/wheat cropping sequence and fertilizer use on soil properties and crop yields in a sodic soil. *Field Crops Research*, *21*(3–4), 277–287.
Tao, F., Zhang, Z., Xiao, D., Zhang, S., Rötter, R. P., Shi, W., et al. (2014). Responses of wheat growth and yield to climate change in different climate zones of China, 1981–2009. *Agricultural and Forest Meteorology*, *189-190*(189), 91–104.
Tao, F. L., Yokozawa, M., & Zhang, Z. (2009). Modelling the impacts of weather and climate variability on crop productivity over a large area: A new process-based model development, optimization, and uncertainties analysis. *Agricultural and Forest Meteorology*, *149*, 831–850.
Tardieu, F., Granier, C., & Muller, B. (1999). Modelling leaf expansion in a fluctuating environment: Are changes in specific leaf area a consequence of changes in expansion rate? *New Phytologist*, *143*, 33–43.
Tian, H. (2002). Dynamics of the terrestrial biosphere in changing global environments: Date, models and validation. *Acta Geographica Sinica*, *57*(4), 379–388.
Tian, H., Chen, G., Lu, C., Xu, X., Hayes, D. J., Ren, W., et al. (2014). North American terrestrial CO_2 uptake largely offset by CH_4 and N_2O emissions: Toward a full accounting of the greenhouse gas budget. *Climatic Change*, *129*, 413–426.
Tian, H., Lu, C., Ciais, P., Michalak, A. M., Canadell, J. G., Saikawa, E., et al. (2016). The terrestrial biosphere as a net source of greenhouse gases to the atmosphere. *Nature*, *531*(7593), 225–228. https://doi.org/10.1038/nature16946

Tian, H., Lu, C. Q., Melillo, J., Ren, W., Huang, Y., Xu, X. F., et al. (2012). Food benefit and climate warming potential of nitrogen fertilizer uses in China. *Environmental Research Letters*, *7*, 044020. https://doi.org/10.1088/1748-9326/7/4/044020

Tian, H. Q., Chen, G. S., Liu, M. L., Zhang, C., Sun, G., Lu, C., et al. (2010). Model estimates of net primary productivity, evapotranspiration and water use efficiency in the terrestrial ecosystems of the southern United States during 1895–2007. *Forest Ecology and Management*, *259*(7), 1311–1327. https://doi.org/10.1016/j.foreco.2009.10.009

Tian, H. Q., Chen, G. S., Lu, C. Q., Xu, X. F., Ren, W., Zhang, B., et al. (2015). Global methane and nitrous oxide emissions from terrestrial ecosystems due to multiple environmental changes. *Ecosystem Health and Sustainability*, *1*(1), 4. https://doi.org/10.1890/EHS14–0015.1

Tian, H. Q., Liu, M. L., Zhang, C., Ren, W., Xu, X. F., Chen, G., et al. (2010). The Dynamic Land Ecosystem Model (DLEM) for simulating terrestrial processes and interactions in the context of multifactor global change. *Acta Geographical Science*, *65*(9), 1027–1047.

Tian, H. Q., Melillo, J., Lu, C. Q., Kicklighter, D., Liu, M., Ren, W., et al. (2011). China's terrestrial carbon balance: Contributions from multiple global change factors. *Global Biogeochemical Cycles*, *25*, GB1007. https://doi.org/10.1029/2010GB003838

Tian, H. Q., Ren, W., Tao, B., Sun, G., Chappelka, A., Wang, X., et al. (2016). Climate extremes and ozone pollution: A growing threat to China's food security. *Ecosystem Health and Sustainability*, *2*(6), 1–10.

Tian, H. Q., Xu, X. F., Lu, C. Q., Liu, M., Ren, W., Chen, G., et al. (2011). Net exchanges of CO_2, CH_4, and N_2O between China's terrestrial ecosystems and the atmosphere and their contributions to global climate warming. *Journal of Geophysical Research*, *116*, G02011. https://doi.org/10.1029/2010JG001393

Tian, H. Q., Yang, Q. C., Najjar, R. G., Ren, W., Friedrichs, M. A. M., Hopkinson, C. S., & Pan, S. F. (2015). Anthropogenic and climatic influences on carbon fluxes from eastern North America to the Atlantic Ocean: A process-based modeling study. *Journal of Geophysical Research: Biogeosciences*, *120*, 757–772. https://doi.org/10.1002/2014JG002760

Tjoelker, M. G., Volin, J. C., Oleksyn, J., & Reich, P. B. (1995). Interaction of ozone pollution and light effects on photosynthesis in a forest canopy experiment. *Plant, Cell and Environment*, *18*, 895–905.

Uehara, G., & Tsuji, G. Y. (1991). Progress in crop modelling in the IBSNAT Project. In R. C. Muchow, & J. A. Bellamy (Eds.), *Climatic risk in crop production: Models and management in the semi-arid tropics and subtropics*, (pp. 143–156). Wallingford: CAB International.

Wang, E. L., & Engel, T. (2002). Simulation of growth, water and nitrogen uptake of a wheat crop using the SPASS model. *Environmental Modelling & Software*, *17*, 387–402.

Wang, X., Wang, Z. H., & Li, S. X. (2003). The effect of nitrogen fertilizer rate on summer maize yield and soil water-nitrogen dynamics. *Acta Ecologica Sinica*, *36*, 1469–1475.

Wei, L., Yi, S., Hua, Z., Jin, Y., & Guo-Hong, H. (2007). Greenhouse gas emissions from northeast China rice fields in fallow season. *Pedosphere*, *17*(5), 630–638.

Wei, X., Velde, M. V. D., Holman, I. P., Balkovic, J., Lin, E., Skalský, R., et al. (2014). Can climate-smart agriculture reverse the recent slowing of rice yield growth in China? *Agriculture Ecosystems & Environment*, *196*(196), 125–136.

Wheeler, T. R., Craufurd, P. Q., Ellis, R. H., Porter, J. R., & Vara Prasad, P. V. (2000). Temperature variability and the yield of annual crops. *Agriculture, Ecosystems and Environment*, *82*, 159–167.

Wieder, W. R., J. Boehnert, G. B. Bonan, and M. Langseth (2014). Regridded harmonized world soil database v1.2. Data set, Oak Ridge: Tennessee Oak Ridge National Laboratory Distributed Active Archive Center. [Retrieved from http://daac. ornl.gov].

Wittig, V. E., Ainsworth, E. A., & Long, S. P. (2007). To what extent do current and projected increases in surface ozone affect photosynthesis and stomatal conductance of trees? A meta-analytic review of the last 3 decades of experiments. *Plant, Cell and Environment*, *30*, 1150–1162.

Wolfe, D. W., Henderson, D. W., Hsiao, T. C., & Alvino, A. (1988). Interactive water and nitrogen effects on senescence of maize. II. Photosynthetic decline and longevity of individual leaves. *Agronomy Journal*, *80*, 865–870.

Xiao, Y., Xie, G., Lu, C., Ding, X., & Lu, Y. (2005). The value of gas exchange as a service by rice paddies in suburban Shanghai, PR China. *Agriculture Ecosystems & Environment*, *109*(3-4), 273–283.

Xu, X. F., Tian, H. Q., Zhang, C., Liu, M. L., Ren, W., Chen, G. S., et al. (2010). Attribution of spatial and temporal variations in terrestrial methane flux over North America. *Biogeosciences*, *7*(11), 3637–3655.

Yan, H. M., Cao, M. K., Liu, J. Y., Zhuang, D. F., Guo, J. K., & Liu, M. L. (2005). Characterizing spatial patterns of multiple cropping system in China from multi-temporal remote sensing images. *Trans. CSAE*, *21*(4), 85–90.

Yang, B., Xiong, Z., Wang, J., Xu, X., Huang, Q., & Shen, Q. (2015). Mitigating net global warming potential and greenhouse gas intensities by substituting chemical nitrogen fertilizers with organic fertilization strategies in rice-wheat annual rotation systems in China: A 3-year field experiment. *Ecological Engineering*, *81*, 289–297.

Yang, Q. C., Tian, H., Li, X., Tao, B., Ren, W., Chen, G., et al. (2014). Spatiotemporal patterns of evapotranspiration along the North American east coast as influenced by multiple environmental changes. *Ecohydrology*, *8*(4), 714–725.

Yang, X., Shang, Q., Wu, P., Liu, J., Shen, Q., Guo, S., & Xiong, Z. (2010). Methane emissions from double rice agriculture under long-term fertilizing systems in Hunan, China. *Agriculture Ecosystems & Environment*, *137*(3-4), 308–316.

Yu, Q., Saseendran, S. A., Ma, L., Flerchinger, G. N., Green, T. R., & Ahuja, L. R. (2006). Modeling a wheat–maize double cropping system in China using two plant growth modules in RZWQM. *Agricultural Systems*, *89*(2–3), 457–477.

Zhai, L. M., Liu, H. B., Zhang, J. Z., Huang, J., & Wang, B.-r. (2011). Long-term application of organic manure and mineral fertilizer on N_2O and CO_2, emissions in a red soil from cultivated maize-wheat rotation in China. *Journal of Integrative Agriculture*, *10*(11), 1748–1757.

Zhang, A., Bian, R., Hussain, Q., Li, L., Pan, G., Zheng, J., et al. (2013). Change in net global warming potential of a rice-wheat cropping system with biochar soil amendment in a rice paddy from China. *Agriculture Ecosystems & Environment*, *173*(8), 37–45.

Zhang, B., Tian, H., Ren, W., Tao, B., Lu, C., Yang, J., et al. (2016). Methane emissions from global rice fields: Magnitude, spatio-temporal patterns and environmental controls: Methane emissions from global rice field. *Global Biogeochemical Cycles*, *30*, 1246–1263. https://doi.org/10.1002/2016GB005381

Zhang, X. K., Meinke, H., Devoil, P., van Laar, H. H., Bouman, B., & Abawi, Y. (2004). Simulating growth and development of lowland rice in APSIM. In Proceedings of 4th international crop science conference, Brisbane. Retrieved from http://www.cropscience.org.au/icsc2004/poster/2/8/1212_zhang.htm

Zhang, Y., Feng, L., Wang, E., Wang, J., & Li, B. (2012). Evaluation of the APSIM-wheat model in terms of different cultivars, management regimes and environmental conditions. *Canadian Journal of Plant Science*, *92*(5), 937–949.

Zhao, W., Bing, L., & Zhang, Z. (2010). Water requirements of maize in the middle Heihe River basin, China. *Agricultural Water Management*, *97*(2), 215–223.

Zhou, J. B., Wang, C. Y., Zhang, H., Dong, F., Zheng, X. F., Gale, W., & Li, S. X. (2011). Effect of water saving management practices and nitrogen fertilizer rate on crop yield and water use efficiency in a winter wheat–summer maize cropping system. *Field Crops Research*, *122*(2), 157–163.